

Nuclear Fuel Behaviour under RIA Conditions

Authors

Marek Stepniewski
Peter Rudling
ANT International

and

Lars Olof Jernkvist
Quantum Technologies AB

With technical contributions from

Friedrich Garzarolli
Ron Adamson
Tahir Mahmood
Alfred Strasser
Charles Patterson

Reviewer

Nicolas Waeckel



A.N.T. INTERNATIONAL®

© February 2023


Advanced Nuclear Technology International
Spinnerivägen 1, Mellerta Fabriken plan4, SE-448 50 Tollerød,
Sweden

info@antinternational.com
www.antinternational.com

Disclaimer

The information presented in this report has been compiled and analysed by Advanced Nuclear Technology International Europe AB (ANT International®) and its subcontractors. ANT International has exercised due diligence in this work but does not warrant the accuracy or completeness of the information. ANT International does not assume any responsibility for any consequences as a result of the use of the information for any party, except a warranty for reasonable technical skill, which is limited to the amount paid for this assignment by each Project programme member.

Quality-checked and authorized by:

A handwritten signature in black ink, appearing to read 'Peter Rudling', is centered on the page.

Mr Peter Rudling, Chairman of the Board of ANT International

Contents

| | |
|--|-------------|
| Executive Summary | IV |
| 1 Introduction | 1-1 |
| 1.1 Historical background to reactivity-initiated accidents and research | 1-1 |
| 1.2 Consequences of reactivity-initiated accidents | 1-2 |
| 1.3 Scope and outline of the report | 1-4 |
| 2 Overview of RIA scenarios | 2-1 |
| 2.1 Overview of reactivity insertion events | 2-1 |
| 2.1.1 Control system failures | 2-1 |
| 2.1.2 Control rod ejections | 2-1 |
| 2.1.3 Coolant/moderator effects | 2-2 |
| 2.2 Expected power pulse characteristics for various accident scenarios | 2-3 |
| 2.2.1 Pulse width and pulse shape | 2-4 |
| 2.2.2 Pulse amplitude | 2-6 |
| 2.3 Summary | 2-8 |
| 3 Overview of damage phenomena | 3-1 |
| 3.1 Types of damage to fuel and cladding | 3-1 |
| 3.2 Phenomena with influence on core coolability | 3-3 |
| 3.2.1 Cladding tube ballooning | 3-4 |
| 3.2.2 Fuel rod fragmentation and fuel dispersal | 3-4 |
| 3.3 Fuel-coolant interaction | 3-6 |
| 3.3.1 Thermal to mechanical energy conversion | 3-6 |
| 3.3.2 Coolant pressure pulses | 3-8 |
| 3.4 Summary | 3-9 |
| 4 Integral RIA simulation tests and separate effect tests | 4-1 |
| 4.1 Integral RIA simulation tests | 4-1 |
| 4.1.1 Overview of pulse reactor tests | 4-1 |
| 4.1.2 Summary of results from tests on fresh fuel rods | 4-9 |
| 4.1.3 Summary of results from tests on pre-irradiated fuel rods | 4-12 |
| 4.2 Separate effect tests | 4-20 |
| 4.2.1 Cladding mechanical properties | 4-20 |
| 4.2.2 Cladding-to-coolant transient heat transfer | 4-27 |
| 4.2.3 Fuel-coolant interaction | 4-32 |
| 4.3 Summary | 4-32 |
| 5 Cladding failure mechanisms | 5-1 |
| 5.1 Brittle failure | 5-1 |
| 5.1.1 Post-DNB failure-failure mechanism 1a | 5-1 |
| 5.1.2 PCMI: Hydrogen-enhanced PCMI cladding failure-failure mechanism 1b | 5-1 |
| 5.2 Ductile failure: Rod ballooning and burst-failure mechanism 2 | 5-2 |
| 5.3 Fuel melt: Molten fuel-induced swelling PCMI cladding failure-failure mechanism 3 | 5-5 |
| 5.4 Summary | 5-6 |
| 6 Parameters affecting RIA fuel performance | 6-1 |
| 6.1 CZP and HZP | 6-1 |
| 6.1.1 Effect on power pulse characteristics | 6-2 |
| 6.1.2 Effect on propensity for PCMI failures | 6-2 |
| 6.2 Pulse characteristics | 6-4 |
| 6.2.1 Pulse characteristics (power increase rate, enthalpy increase, peak enthalpy, pulse width) | 6-4 |
| 6.3 Fuel parameters | 6-9 |
| 6.3.1 Fuel compositional changes | 6-10 |
| 6.3.2 Pulse characteristics | 6-11 |
| 6.3.3 Radial distribution of power | 6-11 |
| 6.3.4 RIM zone development | 6-12 |
| 6.3.5 Melting temperature | 6-14 |

| | | |
|------------------------------|---|-------------|
| 6.3.6 | Thermal conductivity | 6-14 |
| 6.3.7 | FGR | 6-15 |
| 6.3.8 | Pellet-clad gap | 6-24 |
| 6.4 | Cladding parameters | 6-26 |
| 6.4.1 | Irradiation damage | 6-26 |
| 6.4.2 | Oxide layer thickness | 6-27 |
| 6.4.3 | Hydrogen | 6-27 |
| 6.5 | Summary | 6-36 |
| 7 | Predictive computer codes | 7-1 |
| 7.1 | Core and fuel assembly codes | 7-1 |
| 7.2 | Fuel rod thermomechanical codes | 7-4 |
| 7.3 | Short overview of RIA analysis methods | 7-4 |
| 8 | Examples of energy and failure distribution calculations | 8-1 |
| 8.1 | Control rod ejection accidents in PWRs | 8-1 |
| 8.2 | Control rod drop accidents in BWRs | 8-4 |
| 8.3 | Summary | 8-7 |
| 9 | Licensing/acceptance criteria for RIA | 9-1 |
| 9.1 | US NRC regulations - historical background | 9-4 |
| 9.2 | US NRC regulations - current status | 9-4 |
| 9.2.1 | Fuel cladding failure thresholds | 9-5 |
| 9.2.2 | Transient Fission Gas Release | 9-8 |
| 9.3 | Summary | 9-9 |
| 10 | Accident Tolerant Fuel (ATF) | 10-1 |
| 10.1 | Coated zirconium alloy fuel rod cladding | 10-1 |
| 10.2 | Doped uranium dioxide ceramic fuel pellets | 10-3 |
| Appendix A | Reactor kinetics - an introduction | 1 |
| Appendix B | Pulse reactor tests on pre-irradiated LWR fuel rods | 1 |
| B.1 | SPERT-CDC and TREAT tests | 1 |
| B.2 | PBF tests | 3 |
| B.3 | IGR tests | 4 |
| B.4 | BIGR tests | 5 |
| B.5 | NSRR tests | 9 |
| B.5.1 | Tests on PWR UO ₂ fuel rods | 11 |
| B.5.2 | Tests on BWR UO ₂ fuel rods | 17 |
| B.5.3 | Tests on MOX fuel rods | 23 |
| B.5.4 | Tests on JMTR fuel rods | 27 |
| B.6 | CABRI tests | 28 |
| B.6.1 | Tests on UO ₂ fuel rods | 29 |
| B.6.2 | Tests on MOX fuel rods | 31 |
| B.6.3 | Tests in pressurized water coolant loop | 32 |
| Appendix C | (Information from ZIRAT18 STR on Mechanical Testing Vol. II) | 1 |
| C.1 | Mechanical testing techniques | 1 |
| C.1.1 | Mechanical testing techniques | 3 |
| C.1.2 | Expansion Due to Compression (EDC) | 23 |
| References | | 10-1 |
| Nomenclature | | 10-1 |
| List of Abbreviations | | 10-2 |
| Unit conversion | | 10-5 |

Executive Summary

A reactivity-initiated accident (RIA) is a nuclear reactor accident that involves an unwanted increase in fission rate and reactor power. The immediate consequence of an RIA is a fast rise in fuel power and temperature. The power excursion may lead to failure of the nuclear fuel rods and release of radioactive material into the primary reactor coolant. In severe cases, the fuel rods may be shattered, and large parts of the fuel pellet inventory may be dispersed into the coolant.

Two RIA accident scenarios are of particular interest in the core safety analysis: to facilitate the safety case analysis, control rod ejection accidents in pressurized water reactors (PWRs) and control rod drop accidents in boiling water reactors (BWRs) have been selected as reference cases to cover all the reactivity-initiated accidents that may occur. These are design basis accidents, which are used to define operational safety limits for each reactor type. A control rod ejection accident (CREA) can occur in PWRs by mechanical failure of the control rod drive mechanism. The accident results in rapid reactivity increase in a few fuel assemblies around the ejected control rod due to the local decrease of neutron absorption. The design basis reactivity accident in BWRs is the control rod drop accident (CRDA). The initiating event for this accident is the separation of a control rod blade from its drive mechanism. The separation is assumed to take place when the blade is fully inserted in the core, and the detached blade remains stuck in this position until it suddenly becomes loose and drops out of the core in a free fall. Since the CREA and the CRDA are design basis accidents in PWRs and BWRs, respectively, these accident scenarios have over the years been closely analysed by use of computer codes and models which have been validated on in-pile RIA experiments.

The main safety concerns in RIAs are a possible loss of long-term core coolability, and with a very low probability possible damage to the reactor core then to the reactor pressure boundary as a result of the pressure wave generation in case of fuel coolant interaction during the transient. Damage scenarios with loss of long-term core coolability after an RIA involve loss of coolable fuel geometry, for instance by ballooning or fragmentation (shattering) of the fuel rods. Coolable fuel geometry may also be lost even if a rod-like geometry is preserved, in case large amounts of fuel pellet fragments are dispersed into the coolant under the accident. The dispersed fuel particles may block flow channels and impair long-term cooling, or simply pile up in a configuration not amenable to cooling. If the fuel fragments are dispersed during the course of the reactivity transient, violent fuel-coolant interaction (FCI) may occur and generate harmful pressure waves. Fuel rod failure, i.e., loss of cladding tube integrity, is in itself generally not considered a safety concern, since fuel rod failures do not necessarily imply loss of coolable geometry (or generation of harmful pressure waves in case of fuel fragment dispersal and FCI). Nonetheless, studies of RIA damage phenomena have historically been focused on fuel rod failure. The reason is that fuel rod failure is a prerequisite for loss of coolable core geometry and possible pressure wave generation, and that many regulators require that the number of failed fuel rods in the core should be calculated in evaluations of radiological consequences to design basis RIAs.

The fuel rod behaviour under an RIA is affected by the characteristics of the power pulse, the core coolant conditions, the burnup-dependent state of the fuel rod, and the fuel rod design. Based on the results of integral RIA simulation tests, fuel rod failures are usually divided into:

- Low temperature failures (i.e., low coolant temperature), caused by pellet-cladding mechanical interaction (PCMI). These failures occur in fuel rods with hydride embrittled cladding under the early heat-up phase of the accident.
- High temperature failures, which occur at a later stage of the accident, as a result of film-boiling, degraded clad-to-coolant heat transfer, and a prolonged period with overheated cladding.

Low temperature PCMI-induced cladding failures under RIA may occur in high-burnup fuel rods, but not in fresh or low-burnup rods. The reason is that with increased burnup, 1) the RIA hoop stresses applied to the cladding are enhanced by the initial pellet/cladding gap decreases due to pellet swelling and cladding creep down (due to the system overpressure) and 2) the cladding is embrittled by hydrogen pickup through the waterside corrosion reaction. This failure mode is more likely for accidents that initiate from conditions with low reactor power and/or low coolant temperature (hot zero power plant conditions) than for accidents that occur at full reactor power. The PCMI-induced low temperature failures generally occur at significantly lower fuel enthalpies than high temperature failures.

High temperature fuel rod failures under RIA may occur by three different modes: (i) fuel rod cladding creep ballooning and burst, (ii) oxygen-induced embrittlement and fragmentation at post-Departure from Nucleate Boiling (DNB), and (iii) cladding melting. The first of these failure modes can only occur if there is a substantial gas overpressure in the fuel rod. Post-DNB brittle fracture of the clad material occurs during the re-wetting phase of the overheated heavily oxidised (and thereby embrittled) clad due to the abrupt quenching resulting in large thermal clad stresses. This failure mode was frequently observed in early pulse reactor tests on fresh and low-burnup fuel rods, when the fuel enthalpy reached about $240 \text{ cal}(\text{gUO}_2)^{-1}$, i.e., about $1000 \text{ J}(\text{gUO}_2)^{-1}$. Early acceptance criteria for RIA in light water reactors were based largely on this threshold enthalpy. The cladding melting occurrence is usually associated with an extensive fuel melting caused by rapid temperature increase, which is not limited only to the pellet centreline.

Fuel rod fragmentation and loss of rod-like geometry may result from either PCMI-induced failure or post-DNB brittle fracture of fuel rods or molten cladding. In high-burnup fuel rods, the fuel dispersal is driven by gas-induced fragmentation of the pellet. The risk for pressure pulse generation in the coolant is quantified with the energy conversion ratio, i.e., the ratio of the mechanical energy generated in the coolant to the thermal energy in the dispersed fuel.

Current understanding of the fuel behaviour during reactivity-initiated accidents is based on the results of integral RIA simulation tests, performed on instrumented short-length rodlets in dedicated power pulse reactors, and separate effect tests, carried out in-reactor or ex-reactor on fuel or cladding samples. To date, more than a thousand integral RIA simulation tests have been performed on fresh (un-irradiated) LWR fuel rods, using pulse reactors in the USA, France, Japan, Russia and Kazakhstan. Recent work has been focused on the behaviour of pre-irradiated fuel rods, and over the past 50 years, integral RIA simulation tests have been conducted on about 170 pre-irradiated LWR fuel rods in six different power pulse reactors. The majority of the latter tests were performed on UO_2 fuel rods, but 16 of the tests on pre-irradiated rods involved MOX fuel (12 in NSRR and 5 in CABRI). These pulse irradiation tests have shown that cladding failure occurs at lower fuel enthalpies for pre-irradiated than for fresh fuel rods, and that the susceptibility to PCMI failures increases with increasing fuel burnup. However, this is not a burnup effect but rather related to a cladding fluence effect enhanced by a hydride embrittlement effect. With increased burnup, waterside corrosion of the fuel cladding increases which in turn increases the hydrogen pickup in the cladding. As already mentioned, the PCMI induced failures of pre-irradiated BWR and PWR fuel rods usually occur at an early stage of the power surge, when the cladding temperature is low and the hydrided material is still brittle. The results of integral RIA simulation tests also suggest that the typical failure mode of high-burnup VVER fuel is different from that of PWR and BWR fuels. More precisely, VVER fuel does not exhibit PCMI-induced, low-temperature failures: all reported pulse test failures of pre-irradiated VVER fuel rods are due to cladding ballooning and burst, caused by high temperature deformation. The apparent difference in failure behaviour between high-burnup VVER fuel rods and PWR or BWR rods in pulse irradiation tests are related to lower in-reactor cladding corrosion and related hydriding and possibly fuel pellet design differences between VVER and PWR/BWR fuel rods. Recent tests results show that modern PWR and BWR cladding alloys, which exhibit higher performance in terms of corrosion and hydriding, are behaving similarly to the VVER claddings.

The RIA simulation tests on fresh fuel rods usually result in fuel rod fragmentation and dispersal of fuel particles into the coolant when the peak fuel enthalpy exceeds roughly 1000 Jg^{-1} . Pulse reactor tests on pre-irradiated fuel rods show that fuel may be dispersed into the coolant at significantly lower fuel enthalpy ($400\text{--}500 \text{ Jg}^{-1}$), when the fuel burnup exceeds approximately $40 \text{ MWd}(\text{kgU})^{-1}$. The fuel fragments dispersal occurs in connection with PCMI-type cladding failure while the ballooning and burst type of failure does not lead to significant fuel dispersal in the testing conditions investigated to date mainly because the high burnup test rodlets did not have enough residual reactivity to enable high magnitude pulses. It should be noted that direct application of the results from the pulse irradiation tests to LWR conditions cannot be done since the rod design and test conditions are significantly different from that in LWRs. In addition to integral RIA simulation tests, separate effect tests have been carried out to study the effect of a rapid transient on the cladding mechanical properties, on the cladding-to-coolant heat transfer and on the fuel-coolant interaction under well-controlled conditions.

It can be deduced from RIA simulation experiments in power pulse reactors that the fuel rod behaviour under an RIA is primarily affected by the:

- Core coolant conditions, i.e., the coolant pressure, coolant temperature, and coolant flow rate. With respect to reactivity addition in a PWR, the most severe CREA would occur at hot zero power (HZP) conditions, i.e., at normal coolant temperature and pressure, but with nearly zero reactor power. With respect to reactivity addition in a BWR, the most severe CRDA would occur at cold zero power (CZP) conditions, i.e., at a state with the coolant close to room temperature and atmospheric pressure, and the reactor at nearly zero power. The degree of reactivity addition during CRDA is strongly affected by the coolant subcooling ratio, since vapour generation effectively limits the power transient.
- Characteristics of the power pulse, in particular the amplitude and pulse width. The pulse width in pulse reactor RIA tests shown an inverse relationship with the fuel enthalpy rise (i.e., shorter pulse results in larger fuel enthalpy increases (ΔH)). Differences in pulse width are important for two more reasons: narrower pulse width is known to generate higher stresses in the pellets periphery such enhancing cladding stresses (and risk for PCMI-induced cladding failure), higher transient fission gas releases and higher risk of fine fuel fragmentation).
- Burnup-dependent state of the fuel rod. Among the most important properties are the pre-accident width of the pellet-clad gap. The most severe scenarios for RIA in LWRs take place at zero or very low fuel rod power. The PCMI-induced loading under HZP or CZP RIA depends on pre-transient gap size, which in turn depends on the as-fabricated gap size, in-reactor fuel swelling and clad creep-down. The latter phenomena depend on fuel rod design (e.g., initial rod internal pressure and cladding mechanical properties), reactor operating conditions and fuel residence time in the reactor, which means that the pre-transient gap size varies with burnup.
- The degree of cladding embrittlement (through hydrogen pickup). The degree of embrittlement due to hydride precipitation is dependent on the amount of hydrogen in excess of the solubility limit, as well as on size, orientation and distribution of the hydrides. For the same average hydride content, materials with uniformly distributed hydrides are more ductile than those having local concentrations of hydrides in certain regions. Circumferential hydrides (parallel to the circumferential cladding direction) have only a moderate embrittling effect, since there is no tensile stress in the clad tube radial direction, i.e., in the direction perpendicular to the hydride platelets. However, 'radial' hydrides (perpendicular to the circumferential cladding direction), are much more deleterious, since they are perpendicular to the dominating tensile hoop stress in clad tubes of high-burnup fuel rods. The fraction of these detrimental radial hydrides is larger in recrystallization annealed (RXA) clad materials than in stress relieved (SRA) cladding, independently of their chemical compositions.
- The internal gas overpressure in the fuel rod during the RIA transient. It depends on the initial rod internal pressure, the in-reactor Fission Gas Release (FGR) prior to the RIA and the Transient Fission Gas Release (TFGR) during the RIA. For a given rod internal free volume, the internal gas overpressure has a major effect on the fuel rod cladding strain during RIA only if the cladding temperatures reach high values due to a dry-out/DNB phase, late in the RIA sequence. If cladding temperatures remain low, the increase of the internal pressure by TFGR during the RIA transients plays only a minor role for the cladding deformation.

Consequences of postulated RIAs can be assessed by computational tools, usually by estimating the number of fuel rods that may fail during the accident. These assessments are done in two steps, where the first step involves calculation of the pulse amplitude and the resulting peak fuel enthalpy for each fuel rod in the core, more specifically around the failed control rod. In a second step, the calculated peak fuel enthalpy of each fuel rod is compared to the relevant failure criteria, in which the fuel rod state (burnup, internal gas pressure, clad mechanical properties, etc.) is considered. Results of numerous three-dimensional core kinetics analyses of postulated CREAs and CRDAs show that only 10–20% of the fuel within a typical reactor core experiences significant energy deposition. The energy falls off rapidly with increasing distance from the failed control rod, and except for a 6×6 to 8×8 array of fuel assemblies around the rod, the calculated results suggest that the energy deposition is too low to cause fuel rod failures, even under very severe postulated accidents. The fraction of failed rods in the core inevitably depends on the applied failure criterion, but calculated fractions of failed fuel rods reported in open literature for CREAs and CRDAs, are typically around one percent or zero percent with the latest 3D kinetics calculation tools. It must be noted that the predicted failure or survival of each rod is unaffected by the state of surrounding rods. The possibility of a “domino effect” of the failed rod on the surrounding

fuel rods caused e.g., by the build-up and propagation of coolant pressure pulses due to an energetic fuel-coolant interaction or by the presence of defect fuel rods in the vicinity of the failed control rod, is thus not considered in the calculations but can be assessed separately. It is shown that the pressure pulse is rapidly damped into the surrounding bundle and unlikely to generate additional fuel rod failures.

The main safety concerns relative to RIAs is (i) to lose the core coolable geometry and (ii) to damage the reactor pressure boundary and the core as a result of the pressure wave generated by the failed fuel rods, in certain conditions. Fuel failure, i.e., loss of clad tube integrity, is generally not considered as a safety concern (except in Germany), since fuel failures do not necessarily imply loss of coolable geometry or generation of harmful pressure waves. Nonetheless, RIA experiments and modelling have historically been focused on fuel rod failure, for several reasons:

- Fuel rod failure is a prerequisite for loss of coolable core geometry and pressure wave generation,
- The mechanisms for fuel rod failure are more easily studied, both experimentally and analytically, than those for gross core damage.

As such, a “no fuel failure” approach can be used as a surrogate to avoid considering the post-failure phenomena which are difficult to investigate and simulate.

Regulatory bodies require that the number of failed fuel rods in the core should be calculated to evaluate the radiological consequences in case of RIA transient, as for any design basis accident susceptible to lead to fuel rod failures. Acceptance criteria for fuel behaviour under RIA were established by the United States Nuclear Regulatory Commission (USNRC) in the late seventies, based on results from early RIA simulation tests in pulse reactors on fresh or low irradiated fuel. In early nineties, RIA simulations in the French CABRI test reactor and in the Japanese NSRR on high burnup PWR fuel samples failed at fuel enthalpies significantly lower than governing acceptance limit for fuel failure, the fuel burnup impact on acceptance criteria became a challenge. Some countries worked out their own interim burnup dependent limits while others waited for confirmatory tests results and analysis. Such tests have been conducted in France, Japan and Russia and concluded that high burnup fuel rods fail at lower fuel enthalpies than fresh fuel rods. Moreover, failures of pre-irradiated samples usually occur at an early stage of power surge in simulated RIA scenario, when the cladding temperature is still low. The confirmed increased failure susceptibility for pre-irradiated fuel rods and progresses in knowledge of fuel failure mechanisms invoked some regulatory response. This report, i.e., an updated version of the Special Topic Report (STR) on Nuclear Fuel Behaviour under RIA Conditions, describes in detail the current status of the regulatory acceptance criteria for RIA in the US and briefly summarizes for countries with significant nuclear power generation.

Current report version is based on the former report version published in 2016 but covering timeframe until October 2022. As its predecessor the updated report intend to summarize the current understanding of fuel behaviour under RIA in LWRs (the data comprises foremost PWR and BWR but some VVER data are also involved). This understanding is based on experiments as well as computational analyses and the report includes experimental data and calculated results from state-of-the-art computer analyses and belonging analytical tools, computer codes. Data and results are reviewed, and their applicability is assessed, in particular with regard to high burnup conditions. The fuel pellet material of primary concern is UO_2 , but the report covers also $(\text{U,Pu})\text{O}_2$ mixed oxide (MOX) fuel and gadolinium-bearing burnable absorber fuel. Specific characteristics of the non- UO_2 fuels are discussed, and their behaviour under RIA is compared with that of uranium dioxide fuel.

Although some Accident Tolerant Fuel (ATF) designs reached certain degree of maturity the variety and diversity of new fuel systems as well as very limited access to valuable data from the tests conducted in RIA conditions (including in-pile tests) make it impossible to give a fair comparison with the UO_2 based fuel. For this reason, ATF as a fuel type is considered beyond the scope of this report. However, some evolutionary ATF concepts such as coated zirconium alloy fuel rod cladding and doped uranium dioxide ceramic fuel pellets proposed by most of the fuel vendors can be considered as almost mature products. For some of them, albeit limited, results of material tests as well as transient behaviour tests (including

RIA tests conditions) have been published [OECD, July 2022]. To that extent the impact of coated cladding and doped fuel pellets concepts on RIA analysis are discussed in this report.

1 Introduction

A reactivity-initiated accident (RIA) is a nuclear reactor accident that involves an unwanted increase in fission rate and reactor power. Possible accident scenarios in light water reactors (LWRs) include reactor control system failures and control element ejections, but also events caused by inadvertent changes to the reactor coolant, leading to improved neutron moderation [International Atomic Energy Agency (IAEA), 1993]. The power increase may damage the fuel and, in the most severe cases, can create pressure pulses in the reactor coolant. The main safety concerns relative to RIAs is (i) to lose the core coolable geometry and (ii) to damage the reactor pressure boundary and the core as a result of the pressure wave generated by the failed fuel rods, in certain conditions. To preclude these consequences, some bounding scenarios for reactivity-initiated accidents have been identified by the regulatory bodies as design basis accidents, i.e., they have been selected as reference cases to cover all the other types of reactivity accidents.

In current pressurized water reactors (PWRs) and boiling water reactors (BWRs), which are the two most common types of power generating reactors worldwide [Bodansky, 2004], protection against reactivity-initiated accidents is afforded by engineered safety systems, but also by inherent reactor feedback mechanism. More precisely, the reactors are designed so that an unwanted power rise is rapidly terminated thanks to a fast negative reactivity feedback generated by the coolant temperature increase and steam production during the transient. The negative reactivity feedback limits the peak power and provides time for the engineered safety systems to respond and shut the reactor down. No reactivity-initiated accident with severe consequences has so far occurred in PWR and BWR reactor designs.

1.1 Historical background to reactivity-initiated accidents and research

The first reactivity-initiated accidents occurred in the 1950s and 1960s and concerned the first generation of research reactors [McLaughlin et al, 2000]. Examples are the 1952 accident in the NRX reactor at Chalk River, Canada [Hatfield, 1955], and the 1961 SL-1 accident in Idaho Falls, USA [McKeown, 2003], both of which resulted in severe damage and disruption of the reactor. These early reactivity-initiated accidents led to design improvements, which were implemented in later generations of research reactors and, more importantly, in commercial power generating reactors. The design philosophy was to reduce potential causes for RIAs to a minimum, and if an accident still occurred, to quickly terminate the power surge [Glasstone & Sesonske, 1991]. Moreover, some scenarios for reactivity-initiated accidents were identified by regulatory bodies as part of the design basis accidents (DBA) transients against which the reactor must be designed.

Notwithstanding the lessons learned from early research reactors, reactivity-initiated accidents have still occurred in research reactors, military reactors and civil power generating reactors over the last fifty years. For example, a serious accident occurred on board the K-431 Russian Echo-II nuclear powered submarine at the Chazhma Bay naval facility near Vladivostok, Russia, in August 1985 [Takano et al, 2001]. The accident was caused by inadvertent rapid withdrawal of all control rods during reactor refuelling [Takano et al, 2001], leading to a hefty power pulse, steam explosion and subsequent fire. Ten people were killed immediately upon the explosion, but the radiological consequences of the accident were limited, since the PWR-type reactor core was loaded entirely with fresh fuel when the accident occurred [Takano et al, 2001].

The reactivity-initiated accident that occurred in reactor 4 of the Chernobyl nuclear power plant, Ukraine, on April 26, 1986, is unprecedented with respect to radiological consequences and fatalities [IAEA, 1992]. The reactor, which was of light water graphite moderated pressure tube design (RBMK), was destroyed, and contaminated fallout spread over most of the northern hemisphere. The Chernobyl accident and its severe consequences were due to the fact that RBMK do not benefit of fast negative reactivity feedback like PWRs or BWRs core designs, as above mentioned, and due to the fact that RBMKs are built without any reactor containment [IAEA, 1992]. It should also be noted that the accident occurred under a reactor test, where normal operating guidelines were ignored, and safety systems were deactivated.

The Chernobyl accident prompted new research into reactivity-initiated accidents. Utilities and safety authorities in many countries undertook reviews of potential RIAs in their own power plants, and in the early 1990s, experimental programs were also initiated in France, Japan and Russia to study the behaviour of highly irradiated nuclear fuel under reactivity-initiated accidents. These test programs were primarily intended to check the adequacy of existing regulatory acceptance criteria for RIA, which were based largely on test results for un-irradiated or moderately irradiated fuel because at the time the discharge burnups were lower than 33GWd/t. The extension of the experimental database to higher fuel burnup revealed that high burnup fuel exhibited different failure behaviour than fresh fuel, and that the susceptibility to fuel rod failure increased with increasing burnup.

Since existing acceptance criteria for RIA, in many countries operating nuclear reactors, were based on the United States Nuclear Regulatory Commission (USNRC) fuel burnup independent regulations derived from results of early integral RIA tests in pulse reactors on fresh or low irradiated fuel (in early seventies) revisions of these criteria become obvious. Particularly, when RIA simulations in the French CABRI [Papin J., et al., 2002, 2003 and 2007] and in the Japanese NSRR [Fuketa T., et al., 1995, 1996, 1999 and Udagawa Y., et al., 2014b] on high burnup PWR fuel failed at fuel enthalpies significantly lower than governing acceptance limit for fuel failure determination of a fuel burnup impact on acceptance criteria become a challenge. Some countries worked out their own interim burnup dependent limits [Jernkvist, 2006] others waited for confirmatory tests and studies in CABRI and NSRR test reactors. Such tests have been conducted further in France, Japan and Russia and resulted in a strong conclusion that cladding failure of high burnup fuel rods generally occurs at lower fuel enthalpies than for low burnup fuel rods. Moreover, failures of pre-irradiated samples usually occur at an early stage of power surge in simulated RIA scenario, when the cladding temperature is still low. The confirmed increased susceptibility to failure of high burnup fuel rods and increased knowledge of failure mechanisms invoked regulatory response.

Motivated by these facts revision of the existing acceptance criteria for RIA was expected and supported by the regulators, the nuclear industry and the nuclear plant operators. Some countries have chosen their own rule making process while most of them decided to follow the US NRC initiative. Eventually, the US NRC proposed an update of the RIA acceptance criteria which has been closely reviewed by the other regulatory bodies. Current status of the regulatory acceptance criteria for RIA in the US as well as a brief summary of country specific regulations for countries with significant nuclear power generation is brought further in this report.

These revisions, as well as the experimental programs, are still ongoing. Much of the experimental work is carried out in international programs, and the results are shared through expert meetings and seminars arranged by international organizations, such as the International Atomic Energy Agency (IAEA) and the Nuclear Energy Agency of the Organisation for Economic Co-operation and Development (OECD).

1.2 Consequences of reactivity-initiated accidents

Reactivity initiated accidents lead to a fast rise in fuel power and temperature, which may cause failure of the nuclear fuel rods and release of radioactive material into the primary reactor coolant. This material comprises gaseous fission products as well as fuel pellet solid fragments. In severe cases, the fuel rods may be shattered, and large parts of the fuel pellet inventory dispersed into the coolant. The expulsion of hot fuel into water has potential to cause rapid steam generation and pressure pulses, which could damage nearby fuel assemblies, other core components, and possibly also the reactor pressure vessel. The current understanding of these damage mechanisms is based on RIA simulation tests, carried out on short-length fuel rods in dedicated pulse irradiation reactors. To date, more than a thousand pulse irradiation tests of this kind have been carried out on fresh (as-received un-irradiated) fuel rods, and about 150 tests have been done on pre-irradiated samples.

The pulse irradiation tests have shown that fuel rods may fail by several damage mechanisms, depending on the characteristics of the thermal-mechanical loading and the state of the fuel: the thermal-mechanical loading depends on the accident scenario, while the state of the fuel depends mainly on fuel burnup and the reactor operating conditions when the accident occurs. A general observation from the tests is that the degree of fuel rod damage correlates with the peak value of the radial fuel pellet specific enthalpy and the pulse width; the higher the enthalpy and the narrower the

pulse width, the more extensive is the damage. The fuel specific enthalpy, i.e., the radial enthalpy per unit mass of the fuel pellet material, is therefore a fundamental parameter in discussions of reactivity-initiated accidents. As long as the fuel is in solid state, its specific enthalpy, h_f is simply calculated from the fuel temperature, T_f through

Equation 1-1:
$$h_f(T_f) = \int_{T_0}^{T_f} c_f(T) dT$$

where c_f is the specific heat capacity of the solid fuel and T_0 is a reference temperature at which $h_f=0$. In this report, we use $T_0=273\text{K}$. Terminology in engineering literature is a bit slack, and the word “specific” in specific fuel enthalpy is mostly left out for brevity.

All over the document both units for fuel enthalpy are used $\text{cal}(\text{gUO}_2)^{-1}$ and $\text{J}(\text{gUO}_2)^{-1}$, the first one is traditional and widely used in the literature devoted RIA and the other is corresponding SI unit. Sometimes fuel enthalpy or fuel enthalpy increase values are given in both units however not always. The last part of this report comprises unit conversion tables, among others for enthalpy, which allows for easy recalculation of a given in the report enthalpy value to asked units.

Pulse irradiation tests generally show that cladding failure occurs at lower fuel enthalpies for irradiated than for fresh fuel rods, and that the susceptibility to failure increases with increasing fuel burnup and cladding fluence. This is due to two different mechanisms:

1. The first one is related to the formation (i.e., typically at Burnup > 45GWd/t rod average) of the High Burnup Structure (HBS) at the periphery of the fuel pellets. This rim zone concentrates fission products (i.e., Pu and intergranular fission gas bubbles). During an RIA event the injected reactivity is concentrated in this HBS rim zone which heats up very quickly. If the pulse width is narrow enough, heat conduction is insufficient to prevent rapid thermal expansion of the periphery of the fuel pellet which in turn generates high hoop stresses in the cladding. This expansion might be enhanced by the pressurization of the intergranular bubbles present in the rim zone (i.e., high burnup rim effect).
2. In addition to this fuel pellet related phenomenon, the mechanical resistance of the cladding might be impaired by in-reactor waterside corrosion and its related hydriding. Indeed, for certain alloys, the hydrogen pick-up fraction is sufficient to embrittle the cladding either through the formation of hydride blisters (i.e., in cladding cold spots generated by localized corrosion layer spallation or at the pellet/pellet interfaces), or the formation of radial hydrides. Hydrides blisters were observed on high burnup fuel rods with Zr4 claddings while radial hydrides are more frequent in Zr2 cladding.

Moreover, failures of high burnup fuel rods usually occur at an early stage of the power surge when the cladding temperature is still low. The increased susceptibility to failure and the change from high temperature failures to a low-temperature failure mode are attributed to the combined effects of cladding tube embrittlement (i.e., cladding hydrogen content) and aggravated pellet-cladding mechanical interaction in high-burnup fuel rods (i.e., level of rim effect and pulse width). In-pile RIA tests analysis shows that the high burnup cladding embrittlement is the primary parameter to consider assessing the fuel rod failure probability.

Regulatory acceptance criteria for reactivity-initiated accidents are commonly defined in terms of limits on the radially averaged fuel pellet specific enthalpy, or the increase of this parameter during the accidental transient. The acceptance criteria vary with country and reactor type, but regulatory authorities usually postulate two kinds of enthalpy limits: (i) a definite limit for core damage, which must not be transgressed at any axial position in any fuel rod in the core, and (ii) a fuel rod failure threshold, that define whether a fuel rod should be considered as failed or not in calculations of radioactive release (source term and radiological consequence analysis). The core damage limit is to ensure integrity of the reactor coolant pressure boundary and maintenance of core coolability in the event of an accident, and it is generally formulated so that gross fuel rod shattering and mechanical energy generation by fuel-coolant interaction is precluded under any accident scenario. The concern is that the generation of a coolant pressure pulse and its consequences on the neighbour structures are

difficult to simulate. If the analysis cannot demonstrate the harmlessness of the fuel rods failures in terms of long-term core coolability, there may be a legitimate need to use a non-failure criterion. On the other hand, the fuel rod failure threshold, which is not a deterministic failure limit has to be considered as an indicator and additional assessments are requested. In DBAs (Design Basis Accidents), limited fuel failures are generally tolerated if it can be demonstrated that their consequences are manageable (i.e., in terms of radiological consequences but also in terms of thermo-mechanical consequences). In addition, the enthalpy threshold for fuel rod failure is often supplemented with acceptance criteria regarding other parameters of importance to cladding failure, such as the cladding-to-coolant local critical heat flux (DNBR) or the fuel rod internal gas overpressure threshold. Reactor operators must verify that these acceptance criteria are met for the various postulated accident scenarios using validated calculation codes and methods.

1.3 Scope and outline of the report

This report Special Topic Report (STR) on Nuclear Fuel Behaviour under RIA Conditions, which is based on the former report version also intend to summarize the current understanding of fuel behaviour under RIA in LWRs (the data comprises foremost PWR and BWR but some VVER¹ data are also involved). This understanding is based on experiments as well as computational analyses and the report includes experimental data and calculated results from state-of-the-art computer analyses and belonging analytical tools, computer codes. Data and results are reviewed, and their applicability is assessed, in particular regarding high burnup conditions. The fuel pellet material of primary concern is UO₂, but the report covers also (U,Pu)O₂ mixed oxide (MOX) fuel and gadolinium-bearing burnable absorber fuel. Characteristics of the non-UO₂ fuels are discussed, and their behaviour under RIA is compared with that of uranium dioxide fuel.

Although some Accident Tolerant Fuel (ATF) designs approach certain degree of maturity the variety and diversity of new fuel systems as well as very limited access to valuable data from the tests conducted in RIA conditions (including in-pile tests) make it impossible to give a just comparison with the UO₂ based fuel. For this reason, ATF as a fuel type is considered beyond the scope of this report. However, some evolutionary modifications of the existing fuel systems denoted briefly as coated zirconium alloy fuel rod cladding and doped uranium dioxide ceramic fuel pellets introduced by established fuel vendors resulted in mature products, which, to a limited extent, however, are already commercialized. For some of them, albeit limited, results of material tests as well as transient behaviour tests (including RIA conditions) have been published [OECD, Juli 2022]. To that extent it is possible at this time that type of ATF is described in this report (Section 10).

The report includes experimental data and calculated results from state-of-the-art computer analyses, published in open literature up to mid-2022. These data and results are reviewed, and their applicability is assessed, in particular regarding high burnup conditions. The report also provides a review of current as well as projected regulatory acceptance criteria for reactivity-initiated accidents in countries with significant nuclear power generation.

The outline of the report is as follows:

Section 2 deals with scenarios for reactivity-initiated accidents in major types of reactors. Emphasis is placed on control rod ejection accidents in pressurized water reactors and control rod drop accidents in boiling water reactors, which are classified as design basis accidents and deemed to be the most challenging RIA scenarios for the reactor types mentioned. The power pulses caused by these accidents are discussed regarding their shape, width, and amplitude. Additional information and a brief introduction to fundamental concepts of reactor kinetics are provided in Appendix A.

Section 3 provides an overview of damage phenomena that may occur under reactivity-initiated accident, including their consequences. Possible failure modes for the fuel rods are identified, and the conditions under which each failure mode occurs are defined. Moreover, the fuel rod post-failure

¹ Russian type of a PWR usually with hexagonal fuel assemblies.

behaviour is described, with emphasis placed on phenomena influencing core coolability. In this context, we also discuss fuel-coolant interaction, i.e., the conversion of fuel thermal energy into mechanical energy by steam generation, and its potential to cause detrimental pressure pulses in the coolant.

Section 4 summarizes tests and experiments that have been pursued to study the fuel rod behaviour under RIAs. Experimental programs with integral RIA simulation tests, performed in various pulse irradiation reactors, are reviewed. The presentation is focused on reported fuel enthalpy thresholds for cladding failure and fuel dispersal. A distinction is made between test done on un-irradiated and pre-irradiated fuel rods. A more detailed account of the results for pre-irradiated fuel rods is given in Appendix B. In addition, we summarize important separate effect tests with relevance to fuel behaviour in RIAs (i.e., fast transient). These are tests on cladding mechanical properties, cladding-to-coolant transient heat transfer and fuel-coolant interaction phenomena.

Section 5 presents the different mechanisms for cladding failure that may come into play during an RIA, depending on the characteristics of the accident and the state of the fuel.

Section 6 discusses parameters that affect the fuel performance under RIAs. Among these parameters are the power pulse characteristics and the pre-accident coolant conditions in the reactor, but also the burnup dependent state of fuel and cladding.

Section 7 provides a brief overview over the most common in the nuclear industry predictive computer codes used for core-wide and more detailed fuel assembly simulations of RIA and more sophisticated thermo-mechanical fuel rod calculation codes.

Section 8 provides examples of calculated results on core-wide distributions of energy and failed fuel rods under postulated control rod ejection and control rod drop accidents. All studies reviewed in this section were done with state-of-the-art three-dimensional neutron kinetics codes.

Section 9 provides an up-to-date review of currently applied regulatory acceptance criteria for RIA in several countries collected for better comparison in a tabular format. The US NRC regulations are for their importance distinguished by description of the historical background and detailed presentation of its current status.

Section 10 provides a brief introduction to ATF in more detail to evolutionary enhanced ATFs based on current materials used for cladding and pellets and rather limited changes to the fuel rod manufacturing process. Two such ATF technologies are briefly described: (i) coated zirconium alloy fuel rod cladding (ii) doped uranium dioxide ceramic fuel pellets.

2 Overview of RIA scenarios

There is a wide spectrum of scenarios for accidents and events that may result in inadvertent insertion of reactivity in nuclear power reactors. A general overview and classification of these scenarios in light water reactors (LWR) are given in section 2.1. Two accident scenarios are of particular interest: the control rod ejection accident (CREA) in PWRs and the control rod drop accident (CRDA) in BWRs. These are design basis accidents, i.e., postulated events of low probability, which would have serious consequences if they were not inherently accounted for in the design of the reactor and related safety systems. CREA and CRDA are conveniently used in the Safety Analysis Reports (SAR) as surrogates for the various reactivity-initiated accidents that may occur in operation, some of them with higher probability than CREA or CRDA, but with lesser consequences. Section 2.2 deals with the power pulses that are generated in these design basis accidents. We consider the shape, amplitude, and duration of the pulses since these parameters are important to the fuel behaviour in an RIA; see section 6.2.

A very brief introduction to reactor kinetics, relevant to reactivity-initiated accidents, is given in Appendix A. This introduction is strongly recommended for readers that are unfamiliar with the subject, since it provides a background to essential concepts like criticality, reactivity, and reactivity feedback effects.

2.1 Overview of reactivity insertion events

Reactivity insertion events in power reactors can be divided principally into: (i) control system failures, (ii) control element ejections, (iii) events caused by coolant/moderator temperature and void effects, and (iv) events caused by dilution or removal of coolant/moderator poison. In the following subsections, we discuss events belonging to each of these classes for light water reactors. The presentation is based largely on a study of reactivity accidents by the International Atomic Energy Agency [IAEA, 1993].

2.1.1 Control system failures

All major types of power reactors use control elements (rods) for shutdown, and most reactors also use these rods for power control under normal operation. The control rods contain a neutron absorbing material, usually elements such as B, Ag, Cd, In or Hf, which lowers the reactivity when the rods are inserted into the core. Inadvertent withdrawal of these rods, either due to control system faults or operator errors, is a possible cause to reactivity-initiated accidents in all types of power reactors. However, reactor control systems generally place constraints on allowable control rod movements, thereby excluding operator errors if the control systems function well. Further protection is provided by operating limits, known as rod insertion limits (RILs), which put restriction on the reactivity worth¹ of each control element. Hence, should a control rod be inadvertently withdrawn, the RILs ensure that the reactivity addition will be manageable. Events involving inadvertent removal of control rods are generally not classified as accidents but fall into the category of Anticipated Operation Occurrences (AOOs) or Condition II events [IAEA, 1993].

2.1.2 Control rod ejections

A control rod ejection can occur by mechanical failure of the control rod drive mechanism or its housing. As a consequence of the rod ejection, the reactivity of the core is rapidly increased due to decreasing neutron absorption. Since the reactivity addition rates and the resulting power transients are much larger for these events than for other reactivity accident scenarios, control rod ejections belong to the category of design basis accidents in light water reactors. This means that they are postulated, credible with low probability accidents, that are used to establish the design basis for the reactor and to define safety limits for its operation. The postulated accident scenarios for control rod ejections in PWRs and BWRs are further described below.

¹ The change in reactivity that a control rod can produce by changing its axial position in the core.

3 Overview of damage phenomena

3.1 Types of damage to fuel and cladding

As will be shown in section 4.1, it is known from RIA simulation experiments in power pulse reactors that the fuel rod behaviour under an RIA is affected primarily by the following factors [Organisation for Economic Co-operation and Development (OECD), 2010]

- Characteristics of the power pulse, in particular the amplitude and pulse width.
- Core coolant conditions, i.e., the coolant pressure, temperature and flow rate.
- Burnup-dependent state of the fuel rod. Among the most important properties are the pre-accident width of the pellet-cladding gap, the degree of hydrogen pickup through the cladding waterside corrosion, the internal gas overpressure in the fuel rod, and the distribution of solid and gaseous fission products in the fuel pellets.
- Fuel rod design. Parameters of particular importance are the internal fill gas pressure, cladding tube wall thickness, fuel pellet composition ($UO_2/PuO_2/Gd_2O_3$, enrichment) and the fuel pellet geometrical design (solid/annular, initial pellet-clad gap size).

These factors are important to the fuel rod behaviour during an RIA, and they also control what kind of damage may be inflicted to the fuel rod under the accident (Figure 3-1 and Figure 3-2). The rapid increase in power under the RIA leads to nearly adiabatic heating of the fuel pellets, which immediately deform by solid thermal expansion. If the fuel has been operated for some time and gaseous fission products are retained in the fuel, the expansion of the accumulated gas will add to the solid pellet deformation.

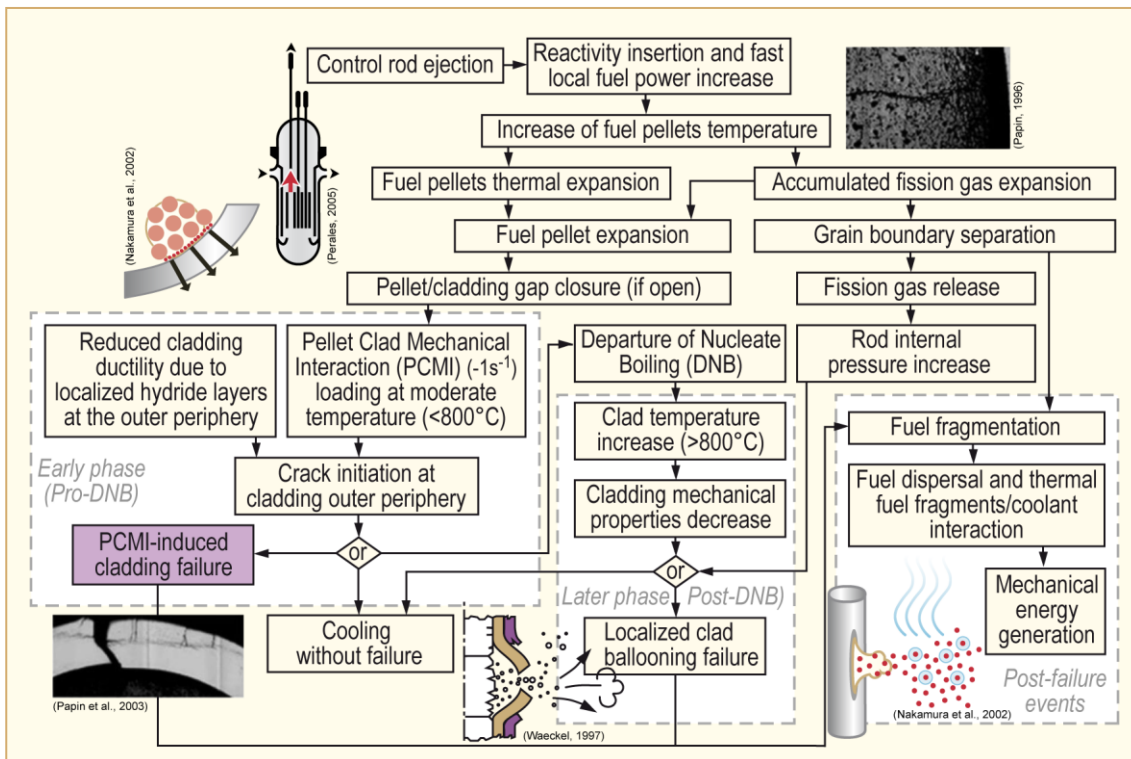


Figure 3-1: Effects of a RIA on fuel [Le Saux et al, 2007].

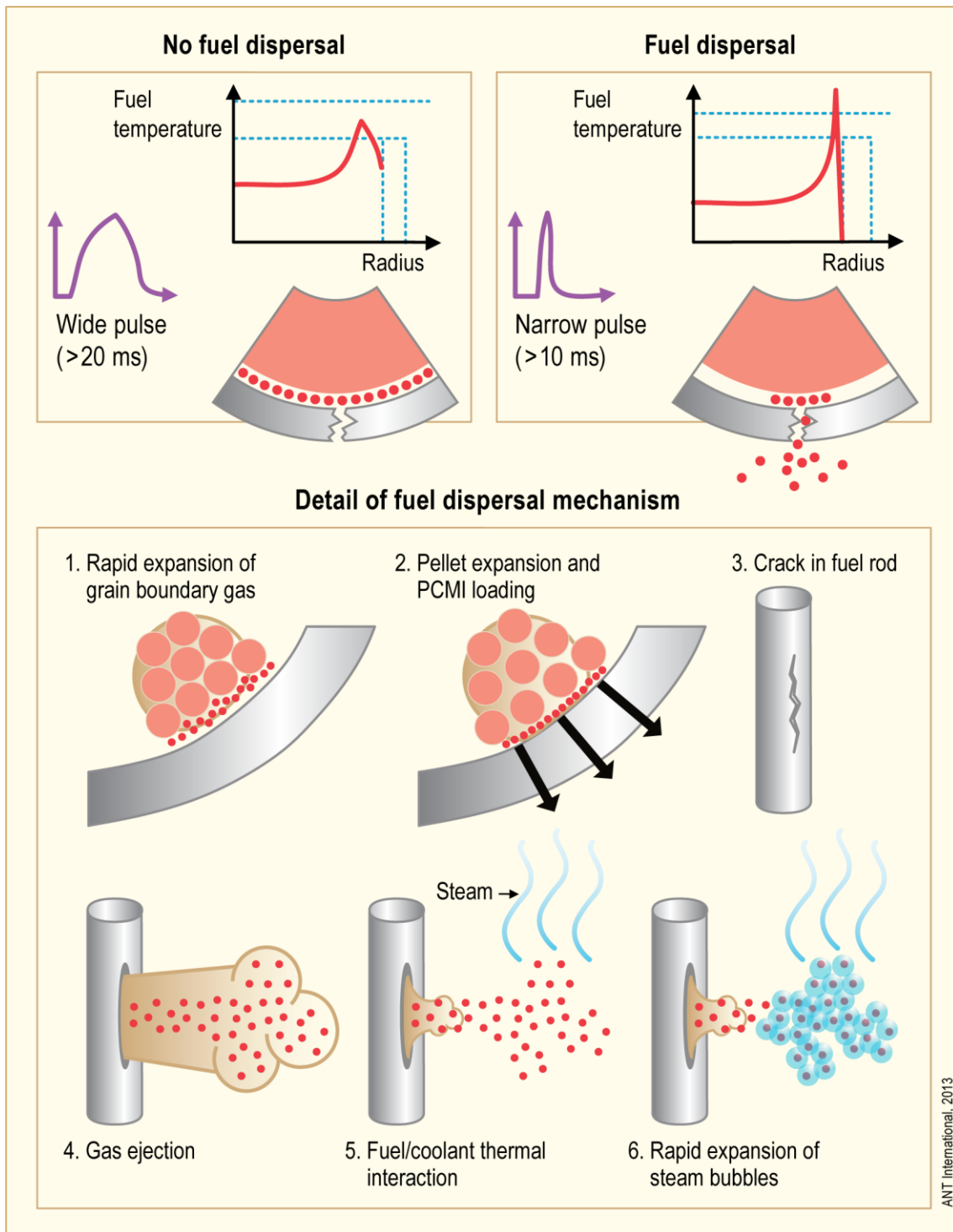


Figure 3-2: Impact of pulse width on high burnup fuel.

In case the pellet-cladding gap is narrow or closed, which is normally the case for high-burnup fuel, pellet-cladding mechanical interaction (PCMI) will lead to rapid and biaxial mechanical loading of the cladding tube. At this early stage of the accident, the cladding material is still at a low temperature, and the thrust imposed by the expanding fuel pellets may therefore cause a partially brittle mode of cladding failure [Chung & Kassner, 1998]. This low-temperature failure mode is commonly observed in pulse irradiation tests on high-burnup fuel rods with embrittled cladding.

At a later stage of the transient, heat transferred from the pellets may bring the cladding to such a high temperature that a boiling crisis occurs. This is sometimes referred to as departure from nucleate

4 Integral RIA simulation tests and separate effect tests

The fuel behaviour during reactivity-initiated accidents has over the years been studied through integral RIA simulation tests, performed on instrumented short-length rodlets in dedicated power pulse reactors, and by separate effect tests, in-reactor or ex-reactor, on fuel or cladding samples. The pulse reactor tests are done at conditions that approximate those expected in power reactors under RIA, and they provide valuable information on the integral fuel rod behaviour under the accident. However, there is currently a lack of experimental facilities, in which integral RIA simulation tests can be carried out in fully representative test conditions. Moreover, the integral tests are costly, and it is also difficult to investigate isolated phenomena and/or the role of particular parameters by in-reactor experiments. Ex-reactor separate effect tests, performed under well-controlled conditions, are therefore needed to investigate e.g., cladding mechanical properties, cladding-to-coolant heat transfer and fuel fission gas release under conditions expected in RIAs. The following subsections provide an overview of RIA integral and separate effect tests, performed up to mid-2022. A more detailed presentation of integral RIA simulation tests on pre-irradiated fuel is given in Appendix B.

4.1 Integral RIA simulation tests

As mentioned in section 1, the main safety concerns in reactivity-initiated accidents are loss of long-term core coolability and possible damage to the reactor pressure boundary and to the core through pressure wave generation. Fuel failure, i.e., loss of cladding tube integrity, is in itself generally not considered a safety concern, since fuel failures do not necessarily imply loss of coolable geometry or generation of harmful pressure waves. Nonetheless, integral RIA simulation tests in dedicated power pulse reactors have historically been focused on fuel rod failure. The reason is that many regulators require that the number of failed fuel rods in the core should be calculated to evaluate the radiological consequences of design basis RIAs. The number of failed fuel rods is also a prerequisite for studying and assessing the impact on core coolability and possible pressure wave generation in case of fuel dispersal and fuel coolant interaction.

4.1.1 Overview of pulse reactor tests

4.1.1.1 Tests on fresh fuel rods

A large number of RIA simulation tests have been performed on fresh (un-irradiated) LWR fuel rods, using pulse reactors in the USA, Japan, Russia and Kazakhstan. These tests, which were carried out predominantly from the sixties to the eighties, can be divided into two groups:

- Tests done to establish thresholds, in terms of peak fuel enthalpy, for cladding failure, fuel dispersal, fuel melting, etc. Since these tests are generally aimed at establishing acceptance criteria for RIAs in power reactors, the tests are done on fuel rods of prevalent commercial design and under conditions that, as closely as possible, resemble those expected for power reactor RIAs.
- Parametric studies, intended to shed light on the fuel behaviour and mechanisms of fuel failure under RIAs, and to generate data needed for validation of computer codes models. The effects of selected parameters are studied by performing series of tests, in which a single parameter of interest is varied at a time. The impact of fuel rod design parameters as well as power pulse characteristics and reactor coolant conditions has been studied in this manner.

Reviews of these early RIA simulation tests on fresh fuel rods are available in literature, e.g. [Asmolov & Yegorova, 1996; Ishikawa & Shiozawa, 1980; Ishikawa et al, 1989; Liimatainen & Testa, 1966; MacDonald et al, 1980]. Table 4-1 summarizes the characteristics of seven pulse reactors, which have been used for RIA simulation tests of fresh LWR fuel rods. The SPERT and PBF reactors have been decommissioned and after an extensive refurbishment TREAT, which has been shut down in 1994, has been taken into operation in 2018 to perform first RIA tests on fresh fuel rods then tests on irradiated fuel rods from 2022. The other reactors listed in Table 4-1 are still in operation. Current status of the

most research reactors in the World can be checked on the IAEA web site [IAEA, <https://www.iaea.org/resources/databases/research-reactor-database-rrdb>]. The type of fuel tested in each reactor is also indicated in Table 4-1. A few fresh fuel rods with MOX [Abe et al, 1992], rock-like oxide (ROX) inert matrix fuel (IMF) [Nakamura et al, 2003] and burnable absorber (BA) [Shiozawa et al, 1988] fuels have been tested, but apart from these exceptions, the tests have been done on rods with UO₂ fuel. The UO₂ test rods were often, but not always, loaded with fuel pellets enriched to higher fractions of ²³⁵U than typically used in commercial fuel rod designs. This is necessary in some of the pulse reactor facilities to increase the energy deposition to levels where fuel rod fragmentation and melting occur; see section 3.2.2. The enrichment affects the radial distribution of power and temperature in the fuel pellet, and parametric studies in the NSRR have shown that increased enrichment lowers the enthalpy threshold for failure of fresh fuel rods [Ishikawa & Shiozawa, 1980].

Table 4-1: Overview of pulse reactor facilities used for RIA simulation tests on fresh LWR fuel rods. All pulse reactors used light water as coolant.

| | TREAT US | SPERT US | PBF US | IGR KZ | BIGR RU | HYDRA* RU | NSRR JP |
|--|-------------|-------------|-----------|-----------|------------|--------------|------------|
| Test conditions | | | | | | | |
| Coolant temperature [K] | 293 | 293 | 538 | 293 | 293 | 293 | 293–578 |
| Coolant pressure [Mpa] | 0.1 | 0.1 | 6.45 | 0.1–16 | 0.1 | 0.1 | 0.1–16 |
| Coolant flow [ms ⁻¹] | 0 | 0 | 0.5 | 0 | 0 | 0 | 0–1.8 |
| Pulse width [ms] | 350–1000 | 13–31 | 11–16 | 100–1000 | 2–3 | 4–8 | 4–7 |
| Test rods | | | | | | | |
| Rod type | BWR | BWR | PWR | VVER | VVER | VVER | BWR PWR |
| Active length [mm] | 140–240 | ≈ 130 | ≈ 1000 | ≈ 150 | ≈ 150 | ≈ 150 | ≈ 130 |
| * The full name for the Russian HYDRA reactor is IIN-3M GIDRA. | | | | | | | |
| ANT International, 2016 | | | | | | | |

4.1.1.2 Tests on pre-irradiated fuel rods

A total of about 150 RIA simulation tests has under the past four decades been carried out on pre-irradiated LWR fuel rods. Most of these tests were done on UO₂ fuel rods, but 14 of the tests pertain to (U,Pu)O₂ mixed oxide fuel. Six different pulse reactors have been used for the testing, and in two of them, RIA simulation tests are still being conducted, as follows:

- SPERT-CDC (Special Power Excursion Reactor – Capsule Driver Core, operated by Idaho National Laboratory, Idaho Falls, ID, USA). Experiments performed in 1969–1970. Reactor decommissioned in 1977-1978.

Special Power Excursion Reactor – Capsule Driver Core. Experiments performed in the United States 1969–1970. The general objective of the tests was to obtain safety-related data on fuel rod behaviour during an RIA [MacDonald et al, 1980]. The experimental program included un-irradiated test rods, as well as test rods pre-irradiated in the Engineering Test Reactor (ETR) to rod average burnups in the range of 1 to 33 MWd/kgU. The SPERT experiments with 132 mm Zry-2 test rods simulated the conditions of a BWR during cold startup (atmospheric pressure at 298K, with no forced coolant flow and zero initial power). The pulse widths were in the range of

5 Cladding failure mechanisms

There are four different fuel cladding failure mechanisms described in the following according to Clifford [Clifford, 2015] – these are the same failure modes as described in Section 3.1. However, to facilitate the understanding of the new proposed NRC regulation, Section 9.2, the grouping of the failure mechanisms is different in this section:

- 1) Brittle Failures:
 - a) Oxygen-induced embrittlement and fragmentation at high-temperature post-Departure from Nucleate Boiling (DNB) occurring at high temperatures,
 - b) Hydrogen-enhanced Pellet Cladding Mechanical Interaction (PCMI) cladding failure occurring at low temperatures,
- 2) Ductile Failure: High-temperature fuel rod cladding creep ballooning and burst occurring at high temperatures,
- 3) Fuel Melt: Molten fuel-induced swelling PCMI cladding failure occurring at high temperatures.

5.1 Brittle failure

5.1.1 Post-DNB failure-failure mechanism 1a

Post-DNB brittle fracture of the clad material occurring during the re-wetting phase of the overheated heavily oxidised (and thereby embrittled) clad due to the abrupt quenching resulting in large thermal clad stresses. At temperatures above 700°C zirconium alloy cladding is rapidly oxidized from both the UO₂-metal reaction on the inside surface and the water-metal reaction on the outside surface. Oxygen absorbed during the oxidation process embrittles the metal and thermal stresses that arise under quenching (re-wetting) may be sufficient to fracture the fuel cladding. Cladding fracture upon quenching from high temperature (HT) is largely controlled by:

- The brittleness of the oxidized material, where the degree of embrittlement depends principally on the oxygen concentration in the transformed β -phase zirconium.
- The magnitude of thermal stress in the cladding. The thermal stress is caused by temperature gradients in the material, and the magnitude of these gradients depends on the quench temperature.

This failure mode was frequently observed in early pulse reactor tests on un-irradiated fuel rods, when the fuel enthalpy reached about 240 cal(gUO₂)⁻¹, i.e., about 1000 J(gUO₂)⁻¹ [Ishikawa & Shiozawa, 1980] and [MacDonald et al, 1980]. Early acceptance criteria for RIA in LWRs were based largely on this threshold enthalpy.

5.1.2 PCMI: Hydrogen-enhanced PCMI cladding failure-failure mechanism 1b

As the burnup increases the failure mode changes from post-DNB (and fuel melting) to PCMI failures during a RIA event for a fuel rod not subjected to DNB (Figure 5-1).

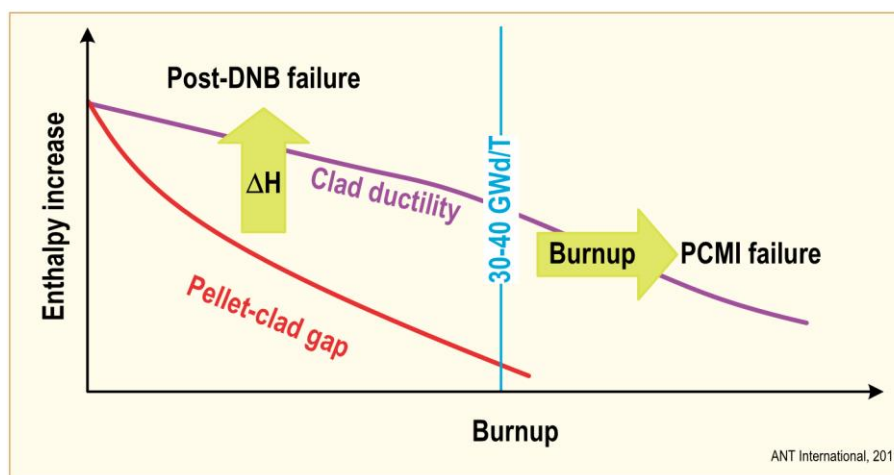


Figure 5-1: Clad failure mechanisms, modified figure according to [Montgomery et al, 2003].

The survival of a high burnup fuel rod under PCMI conditions in a RIA depends on:

- The imposed stress and stress state in the cladding. The stress level depends on the enthalpy increase and pellet-clad gap size prior to the RIA pulse (which decreases with burnup).
- The cladding ductility, which decreases with
 - The clad temperature which in turn is dependent on the pulse width, enthalpy increase of the transient and, heat transfer coefficient between coolant/clad oxide and coolant temperature.
 - The clad hydrogen content, the hydride orientation and distribution.

The PCMI sequence of events in a RIA transient can be summarised as follows:

- The fuel pellet expands rapidly due to thermal expansion during a RIA transient.
- Pellet-cladding gap affects PCMI on RIA:
 - At low burnups the gap is quite large, and a quite high enthalpy increase is needed for gap closure.
 - With increasing burnup, the gap between pellet and cladding decreases during base irradiation due to cladding creep down and fuel swelling, which decrease the enthalpy for gap closure.
 - At high burnup, the gap is closed and consequently, the PCMI will start very early in the transient, as the only space available is the residual gap created by the contraction of the pellet when power was reduced from operating level to zero (for hot-zero-power conditions).

Enthalpy increase after gap closes impose stresses in the cladding, which may eventually fail due to PCMI. The PCMI stresses are generated primary by fuel pellet thermal expansion.

5.2 Ductile failure: Rod ballooning and burst-failure mechanism 2

At a later stage of the transient, heat transferred from the pellets may bring the clad outer surface to such a high temperature that a boiling crisis occurs, whereby a continuous vapour film with very low thermal conductivity forms at the cladding surface. If so, the clad material could remain at a

6 Parameters affecting RIA fuel performance

From RIA simulation experiments in power pulse reactors, the fuel rod behaviour under an RIA is primarily affected by the:

- Core coolant conditions, i.e., the coolant pressure, temperature and flow rate.
- Characteristics of the power pulse, in particular the amplitude and pulse width.
- Burnup-dependent state of the fuel rod. Among the most important properties are the pre-accident width of the pellet-clad gap, the degree of cladding embrittlement (through hydrogen pickup and hydride distribution), the internal gas overpressure in the fuel rod, and the distribution of gaseous and solid fission products in the fuel pellets.

6.1 CZP and HZP

With respect to reactivity addition in a PWR, the most severe CREA would occur at HZP conditions, i.e., at normal coolant temperature and pressure, but with nearly zero reactor power [Agee et al, 1995] and [Nakajima et al, 2002]. In such reactor state conditions the enthalpy variation (ΔH) during the CREA is maximized. On the other hand, if the effect of maximum enthalpy (H_{max}) is investigated (e.g., DNB consequences), at power cases should be considered (even if the enthalpy variation (ΔH) is lower in such cases). In Figure 6-1 it appears that the rod worth¹⁵ decreases with increased power level and with a decrease in control rod insertion within the core.

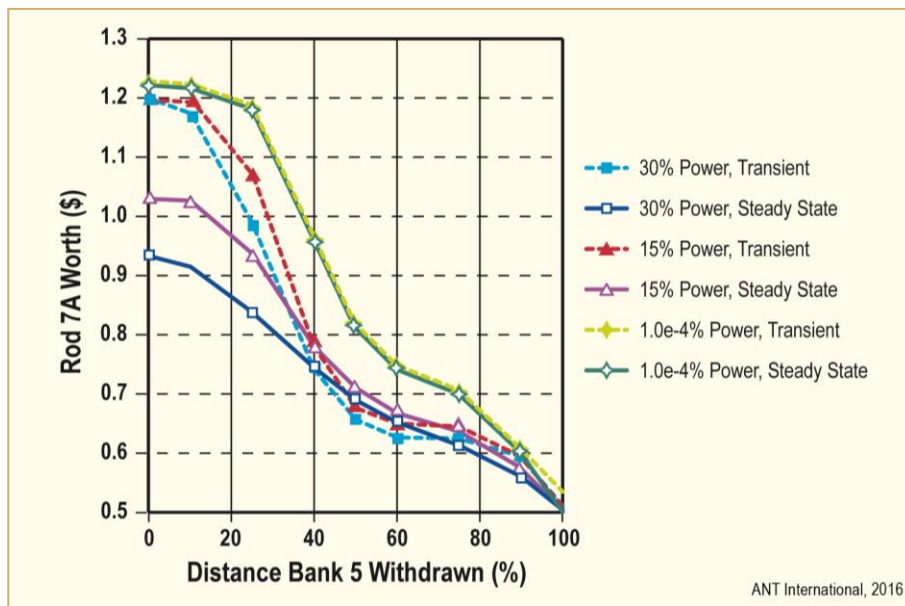


Figure 6-1: Three Mile Island (TMI-1) PWR End of Cycle (EOC) control rod 7a worth variation with power level, bank 5 position, and calculation procedure [Diamond et al, 2001].

With respect to reactivity addition in a BWR, the most severe CRDA would occur at CZP conditions, i.e., at a state with the coolant close to RT and atmospheric pressure, and the reactor at nearly zero power

¹⁵ The control rod worth is roughly proportional to the square of the neutron flux at a given location. The rod worth is a measure for the step decrease (or prompt drop) in the reactivity when a rod is suddenly dropped a known distance into the core (PWR) or inserted into the core (BWR).

[Agee et al, 1995] and [Nakajima et al, 2002]. The degree of reactivity addition during CRDA is strongly affected by the coolant subcooling since vapour generation effectively limits the power transient.

6.1.1 Effect on power pulse characteristics

Table 6-1 provides the estimated values for the pulse width and maximum fuel pellet specific enthalpy under CREAs and CRDAs. The data are taken from realistic and moderately conservative analyses of postulated accident scenarios, which have been carried out with state-of-the-art computer codes and reported in open literature.

Table 6-1: Estimated pulse widths and core-wide maxima of fuel pellet radial average enthalpy and enthalpy increase for various scenarios of CREA and CRDA. The data are compiled from realistic and moderately conservative computer analyses of cores with UO₂ fuel.

| Reactor, accident scenario | Pulse width [ms] | Max fuel enthalpy [J(gUO ₂) ⁻¹] | Max ent. increase [J(gUO ₂) ⁻¹] | Rod worth [10 ⁻⁵] | Literature sources [references] |
|---|--------------------|--|--|--------------------------------|-----------------------------------|
| PWR: | | | | | |
| CREA HZP | 25–65 | 110–320 | 40–250 | 600–940 | [9, 10, 14–18] |
| CREA HFP | 400–4500 | 230–350 | 1–130 | 40–200 | [10, 14, 17, 19–21] |
| BWR: | | | | | |
| CRDA CZP | 45–75 | 140–460 | 130–450 | 700–1300 | [10, 11, 14, 22] |
| CRDA HZP | 45–140 | 160–00 | 90–320 | 600–1300 | [10, 22, 23] |
| HZP: Hot zero power, HFP: Hot full power, CZP: Cold zero power | | | | | |
| ANT International, 2016 | | | | | |

Table 6-1 shows that increased coolant temperatures at CREAs results in both wider pulses and lower maximum fuel enthalpy increases. Thus, a CREA at HZP or a CRDA at CZP results in less margins to fuel failures and fuel dispersal than a CREA at HFP or a CRDA at HZP. Nevertheless, since the pellet-clad gap at HZP is not closed and request some of the enthalpy variation (ΔH) to close the gap (without stressing the cladding), it may happen that partial “at power conditions”, for which the initial gap is naturally closed, and the potential for high enthalpy variation (ΔH) still possible, request specific analysis. To address the same kind of considerations, analysis should be done at different times within the irradiation cycle (beginning of cycle (BOC) or end of cycle (EOC))

6.1.2 Effect on propensity for PCMI failures

The effect of increasing the coolant temperature on the tendency for PCMI failures in a fuel rod during a RIA event can be evaluated by comparing two sibling rods tested both at room temperature (RT) and high temperature (HT).

The first example is the two ZIRLO sibling rods, from Vandellos (VA-1) tested at RT and VA-3 tested at HT (Table 6-2).

7 Predictive computer codes

The most recent and comprehensive overview of computer codes for analysis of different aspects of reactivity-initiated accidents is presented in the State-of-the-Art-Report on RIA prepared by Working Group for Fuel Safety (WGFS) at OECD/NEA [OECD, October 2022]. It includes calculation codes used for in-reactor safety analysis (i.e., predictive codes to simulate the accident in various irradiation conditions) and the detailed thermo-mechanical codes to evaluate and interpretate the RIA simulation tests and transfer their results to in-reactor conditions. This overview includes the following groups of computer codes: (a) codes for neutron-kinetic and thermal-hydraulic analyses, both core-wide and at the level of fuel assemblies, (b) codes devoted to fuel rod behaviour. Since the emphasis in the RIA SOAR [OECD, October 2022] is on fuel behaviour, relatively more attention has been paid to fuel rod thermomechanical codes, for instance by including both a description and an outcome from the fuel rod codes benchmark conducted within the framework of the WGFS activities [OECD, April 2022]. The reader interested in the details can find in the SOAR on RIA [OECD, October 2022] a comprehensive list of computer codes for each code group however with more detailed code descriptions and relevant references. In this report, only limited number of the codes will be mentioned, merely to provide examples of state-of-the-art computational tools for analyses of RIAs. Precedence is given to modern and internationally recognized calculations codes that have a wide user community. It is also important that the calculations codes would have been properly documented, undergone a verification and validation process, and that code uncertainties have been quantified.

7.1 Core and fuel assembly codes

Typically, three groups of codes applied for analysis of reactivity-initiated accidents can be distinguished:

- Codes for generation of homogenised cross-sections
- Codes for core-wide neutron kinetics calculations
- Codes for thermal-hydraulic analysis

The **cross-section codes** calculate probabilities for various neutron reactions, such as absorption, fission or scattering, depending on the neutron energy and the isotopic composition of the material in which the reaction takes place. The first step of a core-wide analysis of the neutron distribution, whether it is a steady-state or a transient analysis, is to condense the cross sections with respect to neutron energy and to homogenise them with respect to space. This is done by means of lattice physics codes, in which the two-dimensional (2D) neutron transport equation is solved within individual fuel assemblies, utilising multi-group transport theory and databases for microscopic cross sections, such as JENDL²⁴, ENDF²⁵ or JEFF²⁶.

User-defined input to the calculations consists of the fuel assembly design, fuel isotopic composition and coolant/moderator properties. Output comprises homogenised cross-sections for the fuel assembly, usually condensed into two neutron energy groups (fast and thermal), delayed neutron data and fuel assembly discontinuity factors. The latter are needed to account for the heterogeneity of the fuel assembly. They improve the accuracy of subsequent core-wide analyses and are also used to reconstruct the neutron flux and power for individual fuel rods within the homogenised assembly.

²⁴ JENDL-4.0 - K. Shibata, et al., "JENDL-4.0: A New Library for Nuclear Science and Engineering", J. Nucl. Sci. Technology. 48(1), 1-30 (2011).

²⁵ ENDF-6 - M.W. Herman, et al., "ENDF-6, Formats Manual, Data Formats and Procedures for the Evaluated Nuclear Data File ENDF/B-VI and ENDF/B-VII", BNL-90365-2009, Dec. 2011

²⁶ JEFF -3.1 - Arjan Koning et al., "The JEFF-3.1 Nuclear Data Library", ISBN 92-64-02314-3

For application in core-wide neutron kinetics analyses, the homogenised cross-sections must be calculated and tabulated as functions of fuel burnup, spectral history, and a number of feedback variables, such as fuel and coolant temperature, coolant density, steam content and boron concentration, and control rod worth and control rod axial positioning. The cross-section's dependence on these variables can be defined either through fitted polynomials, or by use of multidimensional look-up tables. Some widely used lattice physics codes used for generation of homogenised cross-sections are: APOLLO3 (France), CASMO-4 and HELIOS (Sweden), TRITON (US), TVS-M (Russia), WIMS9 (UK).

The procedures for generating the homogenised cross-sections are similar for the codes: starting at the level of a single fuel rod with its surrounding coolant volume, the neutron flux distribution is computed for this unit cell in detail energetically, but only in one dimension spatially – the rod is assumed axisymmetric with infinite axial extension. The cross sections for the unit cell are then condensed into a smaller number of energy groups, typically 10 to 20, and these are then used to compute the two-dimensional distribution of neutron flux at the fuel assembly level. Next, a new condensation is made to get the final set of two-group cross sections for the assembly, which is to be used in the subsequent core-wide analyses.

The **neutron kinetics codes** calculate the space-time variation of neutron flux and power over the entire core in light water reactors by solving the three-dimensional neutron diffusion equation for two neutron energy groups, considering six groups of delayed neutron precursors. The neutron diffusion equation is usually solved on a mesh, in which each node is typically made up of a fuel assembly in the horizontal plane. Since the neutron energy spectrum in a given fuel assembly (node) is little affected by the spectra in adjacent assemblies, the use of only two energy groups in core-wide analyses is justified.

The governing equations for the time-dependent neutron diffusion problem can be solved by various methods, most often, however by means of nodal methods. The nuclear properties as well as the coolant properties are thereby assumed to be uniform within each node, which requires that lattice physics codes are used in a preparatory step to generate homogenised nuclear cross sections and kinetic data for each node. Likewise, the primary results from the calculations are nodal average values, which means that methods for de-homogenisation are needed to extract results for individual fuel rods, such as the fuel enthalpy.

As mentioned in Appendix A, the neutron kinetics in reactor depends on a number of feedback variables, such as fuel temperature and coolant properties, which affect the neutron cross sections. Neutron kinetics codes therefore comprise suitable models for fuel-to-coolant heat transfer and coolant thermal-hydraulics, by which these feedback variables can be calculated. The thermal-hydraulic models are essentially one-dimensional, and they are typically applied to vertical flow channels, each of which is made up of an axial stack of discrete nodes in the neutron kinetics problem. Consequently, thermal-hydraulic boundary conditions must be supplied for the coolant conditions at the top and bottom of the core. Some widely used computer codes for three-dimensional neutron kinetics calculations are: BIPR-8 (Russia), DYN3D (Germany), PANTHER (UK), PARCS, SPNOVA and ANC-K (US), POLCA7 and SIMULATE-3K (Sweden).

The codes for three-dimensional core-wide neutron kinetics calculations described above comprise simple models for core thermal-hydraulics and heat transfer, which makes it possible to run the codes in stand-alone mode. However, there is a current trend to replace these simplified models with more sophisticated methods. This is usually done by integrating a neutron kinetics code with a thermal-hydraulic system analysis code. The aim of the so-called internal coupling is to improve the thermal-hydraulic modelling of the core, but also to gain better modelling consistency between the core and ex-core components of the primary system.

8 Examples of energy and failure distribution calculations

Power pulses expected as a consequence of control rod ejection accidents (CREA) in PWRs and control rod drop accidents (CRDA) in BWRs were discussed in section 2.2, where we concluded that the pulse width is a core-wide parameter, which for large reactivity insertions ($\Delta\rho > \beta$) is approximately proportional to the inverse of the prompt reactivity insertion $\Delta\rho - \beta$. The pulse amplitude, however, is a local property that falls off with increasing distance from the failed control rod, and it also depends on fuel burnup; see section 2.2.2.

To assess the consequences of an RIA, i.e., to estimate the number of failed fuel rods, it is necessary to first calculate the pulse amplitude and the resulting peak fuel enthalpy for each fuel rod.²⁷ The peak fuel enthalpy of each rod is then compared with relevant failure criteria, in which the pre-transient fuel rod state (burnup, internal gas overpressure, cladding corrosion, pellet-cladding gap, conditioning level, etc.) of the fuel rod is considered. A few studies of this kind are available in open literature. More specifically, state-of-the-art computational methods have been used to analyse postulated CREAs and CRDAs, and the distribution of energy and failed fuel rods have been calculated across the reactor core for these accident scenarios. An overview of reported studies on postulated CREAs is given in section 8.1, whereas section 8.2 summarizes analyses of CRDAs. All studies covered in these subsections relate to reactor cores with UO₂ fuel and were done with three-dimensional neutron kinetics codes, but large differences exist as to the postulated accident scenarios and reactivity additions. Moreover, the applied fuel rod failure criteria varied significantly between the reported studies.

8.1 Control rod ejection accidents in PWRs

Table 8-1 summarizes typical computational studies of postulated CREAs, in which calculated results on the distribution of energy and failed fuel rods across the reactor core are presented. All studies in Table 8-1 were done for end-of-cycle core (EOC) conditions, and with two exceptions, they all pertain to CREAs that initiate from hot zero power reactor conditions. These are the most challenging conditions for CREA, design basis accident in a PWR.

²⁷ Here, the peak fuel enthalpy refers to the peak value, with respect to time and axial position, of the radial average fuel enthalpy under the accident.

Table 8-1: Summary of typical computational studies of postulated control rod ejection accidents, in which calculated distributions of energy and failed fuel rods are reported. [OECD, October 2022]

| Core initial conditions | Reactivity insertion ($\Delta\rho/\beta$) | Peak enthalpy increase [$\text{J}(\text{gUO}_2)^{-1}$] | Fraction of failed rods [-] | Investigator [reference] |
|-------------------------|---|--|-----------------------------|--------------------------|
| EOC HZP | 1.89 | 247 | 0 | Nakajima [2002] |
| EOC HZP | 0.88 | 30 | 0 | Dias et al. [1998] |
| EOC HZP | 1.30 | 71 | 0 | Dias et al. [1998] |
| EOC HZP | 1.58 | 143 | 3.6×10^{-2} | Lee et al. [1995] |
| EOC HZP | 2.63 | 439 | - | Marciulescu [2006] |
| EOC HFP | 0.30 | 62 | - | Marciulescu [2006] |
| EOC HFP | 0.23 | 47 | - | Marciulescu [2006] |
| EOC HFP | 0.15 | 83 | 9.0×10^{-3} | Lee et al. [1995] |
| EOC 30% of FP | 1.58 | 112 | 9.0×10^{-3} | Gensler et al. [2015] |
| ANT International, 2016 | | | | |

For illustration, we will consider the study by Nakajima [2002]. This study was done for a typical four-loop PWR, in which the core consisted of 193 fuel assemblies of 17×17 design. The ejection of a fully inserted control rod was postulated at the end of a reactor operating cycle, while the core was held at hot zero power conditions. The reactivity worth of the ejected control rod, $\Delta\rho$, was increased from its realistic value of 6.0×10^{-3} to 8.7×10^{-3} , and penalizing assumptions were also made regarding reactivity feedback effects, in order to increase the energy deposition to the fuel. The calculations were made with the EUREKA-JINS/S three-dimensional neutron kinetics code [Nakajima, 2002].

Figure 8-1 shows the position of the ejected control rod, together with the calculated distribution of energy in terms of peak fuel enthalpy. The highest enthalpy, $78 \text{ cal}(\text{gUO}_2)^{-1}$ or $327 \text{ J}(\text{gUO}_2)^{-1}$, is reached in a first cycle fuel assembly, neighbouring to the assembly from which the control rod is ejected. The fuel assembly loading pattern in the reactor core is shown to the right in Figure 8-1. The calculations show that first cycle fuel assemblies close to the ejected control rod position reach the highest fuel enthalpies, as a consequence of the comparatively high reactivity of low-burnup fuel. It is clear from Figure 8-1 that the calculated peak fuel enthalpy around the ejected control rod decreases rapidly, as the distance from the ejected rod increases. The enthalpy increases by more than $10 \text{ cal}(\text{gUO}_2)^{-1}$ in only 39 of the 193 fuel assemblies; the initial, pre-transient, fuel enthalpy was $19 \text{ cal}(\text{gUO}_2)^{-1}$ throughout the core.

The calculated peak fuel enthalpy increase of individual fuel rods is shown in Figure 8-2. The highest enthalpy increase is experienced by fuel rods in first cycle fuel assemblies, which have a fuel pellet average burnup below $20 \text{ MWd}(\text{kgU})^{-1}$.

9 Licensing/acceptance criteria for RIA

The main safety concerns in RIAs are loss of long-term core coolability and possible damage to the reactor pressure boundary and the core through pressure wave generation. Fuel failure, i.e., loss of clad tube integrity, is in itself generally not considered a safety concern (except in Germany), since fuel failures do not necessarily imply loss of coolable geometry or generation of harmful pressure waves. Nonetheless, RIA experiments and modelling have historically been focused on fuel rod failure, for several reasons:

- Fuel rod failure is a prerequisite for loss of coolable core geometry and as a consequence generation of a coolant pressure pulse, which is too complex to simulate with the standard design calculation tools.
- The mechanisms for fuel rod failure are more easily studied, both experimentally and analytically, than those for gross core damage.
- A number or percentage of fuel rods in the core determined as failed, in accordance with governing rules, should be accounted for in the radiological consequence analysis for RIA.

Acceptance criteria for RIA are usually defined by regulatory authorities however, in some country's acceptance criteria are proposed by the licensees and then approved by regulatory authorities. These criteria form the design basis for reactivity control systems and usually they also define safety limits that must not be transgressed under reactor operation. The acceptance criteria vary with country and reactor type but they are generally formulated to preclude under any accident scenario that energy deposition exceed a destructive level. A limited fuel damage is generally tolerated, at least if the considered accident scenario is judged to occur with very low frequency. The acceptable amount of damage is settled by the requirements to meet regulatory limits on radiation dose to the public, and to ensure integrity of the coolant pressure boundary and long-term coolability of the fuel.

The acceptance criteria are based on the results of RIA simulation tests, conducted in dedicated research reactors. The criteria are commonly defined in terms of limits on the radially averaged fuel pellet specific enthalpy, or the increment of this property during the reactivity-initiated accident. Regulatory authorities usually postulate two kinds of enthalpy limits:

- a definite limit for core damage, which must not be transgressed at any axial position in any fuel rod in the core.
- and fuel rod failure thresholds, that define whether a fuel rod should be considered as failed or not in calculations of radioactive release.

The enthalpy thresholds for fuel rod failure are often supplemented with acceptance criteria for other parameters of importance for cladding failure, such as the clad-to-coolant local heat flux or the fuel rod internal gas overpressure. Reactor operators must verify that these acceptance criteria are met through computer analyses of postulated accident scenarios. Alternatively, fuel vendors or operators may propose design-specific acceptance criteria.

Recently published by OECD/NEA State-of-the-Art-Report on RIA [OECD, October 2022] collect and compare currently applicable national regulatory acceptance criteria and guidance for 12 NEA member countries in Table 9-1 and Table 9-2. Table 9-1 provides a comparison of regulatory acceptance criteria and analytical limits defined to preserve coolable geometry and protect the reactor coolant pressure boundary and reactor internals in these countries. Table 9-2 is a similar comparison of analytical limits used to define the thresholds for different modes of cladding failure. Note that many national regulatory authorities are actively updating analytical limits to capture recent research on high burnup fuel.

Table 9-1: Comparison of regulatory acceptance criteria to preserve coolable geometry, [OECD, October 2022]

| Country | Peak radial average fuel enthalpy [cal/g] | Allowable fuel melting | Additional limits | Allowable fuel damage |
|----------------|---|--|--|---|
| United States | 230 | <10% pellet volume, centerline | -- | Dose limited |
| Switzerland | 230 | No melting | -- | Dose limited |
| Germany | Dictated by precluding PCMI clad failure | Partial melting permitted, if fuel is retained and molten fuel relocation is excluded | -- | None |
| France | 200 for $E_{FA} < 33$ GWd/tU For higher E_{FA} , enthalpy is limited to preclude PCMI clad failure | <10% pellet volume, centerline | Several; see Section F.3 in Appendix F | <10% due to boiling crisis |
| Sweden | Closely follow US NRC criteria and guidance | | | |
| Belgium | Closely follow US NRC criteria and guidance | | | |
| Finland | 230 | Melting of the fuel rod shall be prevented. Local melting in the pellet center is not prohibited, if fragmentation enthalpy is not exceed. | PCT <1 200°C | <10% |
| Czech Republic | 200 for $E_{RA} \leq 50$ GWd/tU, 165 for $E_{RA} > 50$ GWd/tU | No melting | -- | Dose limited |
| Hungary | 230 ¹ | No melting | -- | Dose limited |
| Russia | 200 at $E_{PA} = 0$, decreasing with burnup | No melting | PCT <1 200°C | Dose limited |
| Japan | 230 for $E_{PA} < 30$ GWd/tU, decreasing with higher burnup | No melting | -- | Limit in terms of mechanical energy generation by FCI |
| Korea | 230 | No melting | -- | Dose limited |

E_{FA} / E_{RA} / E_{PA} : Fuel assembly average / Fuel rod average / Fuel pellet average burnup. PCT: Peak cladding temperature.
¹ The limit refers to peak rise of radial average fuel enthalpy during the accident.

10 Accident Tolerant Fuel (ATF)

Accident Tolerant Fuel (ATF) as such is not a subject of this topic report however several sharing points with RIA in the LWRs and reactivity-initiated accident mitigation due to the fuel construction are worth to be mentioned. Nuclear fuel systems are highly complex and have been subject to continuous development over the past 50 years and has reached a stage where it can be safely and reliably irradiated up to 65GWd/tU (assembly average) in commercial nuclear reactors [IAEA, 2014]. All light water reactors (LWRs) around the world are currently using fuel systems comprised of uranium oxide (UO₂) encased within a zirconium-based alloy cladding. Some reactors use uranium-plutonium oxide (MOX) fuels. The oxide fuel-zircaloy system has been optimised over many decades and performs very well under normal operations and anticipated transients however, under some low frequency accidents, is resulting in undesirable core damage if the core cooling system fails. Severe accidents, such as those at the Three Mile Island and Fukushima Daiichi have shown that under such extreme conditions, nuclear fuel will fail and the high temperature reactions between zirconium alloys and water will lead to the generation of hydrogen, with the potential for explosions to occur, damaging the plant further. Particularly noticeable is the acceleration of a different kind of ATF concepts after the Fukushima accident to gain some grace time before the fuel starts to melt (which it will do eventually). The global nuclear industry is leading this development of nuclear fuel with the goal of achieving significantly improved both operational and safety features. The variety of technical solutions, including new materials, have reached different degrees of development and technical maturity, denoted as the technology readiness level (TRL). The number of publications in this field is steadily growing, and so far, it is difficult to single out one dominant direction. A valuable survey of the subject can be found in [IAEA, 2014; Mahmood et al., 2021; OECD, 2018; OECD, July 2022].

Developing fuel systems and new materials that meet the nuclear power industry expectations regarding improved operational performance and enhanced accident tolerance, together with extensive testing and qualification takes a long time, usually between 10 to 20 years to cover the whole burnup range with appropriate testing candidates. Some fuel vendors in order to reduce the time to bring a qualified product to market, went in the direction of evolutionary enhanced ATF that is, stepwise development of the current construction materials for cladding and pellet and rather limited changes to the fuel rod manufacturing process. Two such ATF technologies are described briefly below:

- Coated zirconium alloy fuel rod cladding.
- Doped uranium dioxide ceramic fuel pellets.

10.1 Coated zirconium alloy fuel rod cladding

One solution to further improve the performance of the cladding in normal and accidental conditions is to protect the external surface of the current zirconium alloys through surface treatments such as the deposition of coatings. The concept of improved or coated Zr-alloy claddings has been adopted by many fuel vendors around the world and is considered one of the near-term accident-tolerant fuel (ATF) candidates.

There have been dozens of coating materials proposed and tested around the world, from metallic to fully ceramic coatings, along with a variety of deposition techniques. Cr-based coatings are generally considered the most mature.

In the Technical Opinion Paper [OECD, July 2022] the following coated cladding concepts for LWRs are mentioned as considered by fuel vendors:

- Cr deposited by physical vapour deposition (PVD) – Framatome and TVEL.
- Cr deposited by Cold Spray technique (CS)- Westinghouse
- Cr-based coating deposited by PVD - TVEL.
- Cr-based metallic CrAl coating deposited by arc ion plating - KEPCO Nuclear Fuel (KNF).

- Ceramic fretting/oxidation resistant “ARMOR” coating for BWRs with a publicly unknown composition - GNF
- Cr deposited by several methods (PVD, CS, laser deposition and plasma spraying) - China General Nuclear (CGN).

It should be added that other surface modification concepts are investigated, however, as shown above, the fuel vendors are mainly pursuing Cr-based coated claddings that were found on the basis on the TRL judgement closest to the market. Additionally, summarised attributes of Cr and CrN coated cladding that serve as the starting point when evaluating the impacts on existing nuclear fuel safety and design requirements reported in the public literature are fatigue, CRUD deposition, heat transfer characteristics and pool-boiling critical heat flux (CHF), as well as ballooning, burst and quenching. Some publications, however, show inconsistency in the reported effects.

During normal operations, the main benefits of Cr-coated claddings are expected to be lower waterside corrosion rates, reduced hydrogen uptake, improved wear resistance, and higher thermal creep strength. These properties, seen in the perspective of a potential RIA, should give a significant positive impact on the course and character of the fuel cladding failure.

Under accident conditions, anticipated benefits include enhanced high temperature oxidation resistance resulting in reduced energy release from the exothermic metal-water oxidation reaction, potentially lowering peak cladding temperatures, improved residual post-quench ductility due to less oxygen embrittlement and reduced combustible gas generation. Another important anticipated benefit, clearly important for RIA behaviour, is reduced high temperature creep and ballooning and potentially smaller burst opening size.

Since only outer surface coatings on standard Zr alloys are considered, fuel and cladding interactions are comparable to standard Zr-alloy and UO₂ fuel. Small variations in fuel performance could potentially occur, such as higher pellet-cladding contact pressure due to a cladding with increased strength, but these variations are not significantly different from those which could occur even with a different Zr-alloy cladding and the performance from the perspective of pellet-cladding interaction (PCI) is similar to the traditional Zr-alloy and UO₂ fuel system.

Most of the current reactivity-initiated accident (RIA) limits are set in place to prevent cladding failure due to pellet-to-cladding mechanical interaction (PCMI) or high-temperature post-DNB ballooning and burst. It is a highly dynamic and integrated phenomenon depending on the pellet, cladding, initial and accident conditions. The Cr coating does not significantly change the response of the cladding and therefore the current phenomena are still relevant. However, the values of current fuel enthalpy or rise enthalpy limits are based on RIA tests that have been performed on irradiated and unirradiated fuel rodlets in various research test reactors using uncoated cladding. The impact of the Cr-based coatings on the relevance and applicability of those tests and results, i.e., the values of the limits, should be assessed. It should be also noted that hydrogen in the cladding due to waterside corrosion can embrittle the cladding, which can affect other safety limits such as those for anticipated operational occurrence (AOO) cladding strain, i.e., RIA PCMI cladding failure. For Zr-alloy cladding, the steady-state cladding oxidation and/or hydrogen limits are established to preclude oxide spallation, which has typically been observed above 75-100 µm and/or to limit the mechanical cladding damage due to the oxidation and hydriding. Zirconium oxide spallation can lead to a local cool spot, which acts as a sink for hydrides, creating notably a local, extremely brittle hydride lens. Coating oxide and coating spallation are not expected to result in localised hydrogen concentrations because their removal would lead to a hot spot due to the formation of ZrO₂, which is a thermal insulator. This nevertheless has to be assessed depending on the Cr-coated cladding design. The impact of the coating on hydrogen uptake must be assessed in light of the thin oxide scale and potential permeability of hydrogen through the coating oxide and coating. The current analytical limits are therefore adequate/conservative, but they should be evaluated in light of changes to the corrosion-related processes.

Appendix A Reactor kinetics – an introduction

More than 99% of all neutrons produced in a fission reactor are prompt neutrons, meaning that they are born and emitted directly from the fission process. However, a fraction β of the neutrons are delayed neutrons that stem from decay of unstable fission products. The delay time of these neutrons is about 15 seconds for typical UO_2 fuel. The delayed neutrons are crucial for controlling the reactor power and for maintaining reactor stability. Under steady-state reactor operating conditions, just as many neutrons are produced by fission as are lost by absorption and leakage from the reactor in a given time. The condition for criticality, i.e., for a self-sustaining fission chain reaction to be possible, is that $k_{eff} = 1$. Here, k_{eff} is the effective neutron multiplication factor, i.e., the ratio of neutron production to neutron absorption and leakage. During steady-state reactor operation, the delayed neutrons make the reactor respond slowly to small changes in the neutron balance, which eases reactor power control. As a measure of the neutron balance, the static reactivity, ρ , is defined as the fractional departure from core criticality

$$\text{Equation A-1: } \rho = \frac{k_{eff}-1}{k_{eff}}$$

A positive reactivity thus indicates a move towards supercriticality (power increase), whereas a negative reactivity corresponds to a move towards subcriticality (power decrease). Under reactor operation, the reactivity can be controlled, e.g., by movements of control rods or by addition/removal of soluble neutron absorbers in the coolant or moderator. However, reactivity is also affected by changes in fuel and moderator temperature, and by changes in the moderator steam (void) content. Hence, the reactivity rate of change may be written:

$$\text{Equation A-2: } \dot{\rho} = \dot{\rho}_{CS} + \frac{\partial \rho}{\partial T_f} \dot{T}_f + \frac{\partial \rho}{\partial T_m} \dot{T}_m + \frac{\partial \rho}{\partial \alpha_m} \dot{\alpha}_m$$

where $\dot{\rho}_{CS}$ is the reactivity rate of change induced by reactivity control systems, \dot{T}_f and \dot{T}_m are the rates of temperature change for fuel and moderator, and $\dot{\alpha}_m$ is the rate of change for the moderator vapour phase (void) volume fraction [145, 146]. Of the partial derivatives on the right-hand side of Equation A-2, the fuel temperature (Doppler) coefficient $\partial \rho / \partial T_f$ is always negative, which means that the fuel temperature increase accompanying a rise in reactivity always provides negative feedback, to the benefit of reactor stability. The other partial derivatives, which are usually termed moderator temperature and void coefficients, can be either positive or negative, depending on reactor design and/or operating conditions.

In the exceptional case that the reactivity exceeds the fraction of delayed neutrons, β , the reactor becomes prompt critical, meaning that the reactor is critical on prompt neutrons alone.²⁸ If such a significant reactivity is added suddenly, e.g., by a fast control rod withdrawal, the reactor power will rise rapidly until the negative fuel temperature feedback terminates the power rise within a few hundredths of a second [145]. Additional negative reactive feedback is obtained from coolant heating, and possibly also from coolant void generation, but these effects are much slower than the fuel temperature feedback. In addition to these inherent feedback mechanisms, engineered safety systems will usually also help to terminate the power pulse. These systems are, however, slower than the inherent feedback mechanisms from fuel and coolant temperature.

The adiabatic Nordheim-Fuchs model gives simple analytical expressions for the pulse width and pulse shape under conditions of prompt criticality [Hetrick, 1993; Lewins, 1995]. This is a simple point-kinetic model, in which adiabatic fuel heating and a linear negative fuel temperature feedback on reactivity are

²⁸ The reactivity at which prompt criticality is reached, $\rho = \beta$, is often denoted with the unit dollar (\$). Hence, the reactivity in dollars and cents is defined by ρ/β .

assumed. Other feedback effects, as well as the effects of delayed neutrons, are neglected. According to the model, for a step-like insertion of reactivity $\Delta\rho$, the full width at half maximum (FWHM), τ , of the power pulse is approximately given by

Equation A-3:
$$\tau = \frac{4\cosh^{-1}(\sqrt{2})\Lambda}{\Delta\rho-\beta} = \frac{3.5255\Lambda}{\Delta\rho-\beta}$$

provided that $\Delta\rho > \beta$. Here, Λ is the effective neutron lifetime, i.e., the mean time between the birth of a fission neutron and its subsequent absorption, leading to another fission. This parameter is specific to the fuel and reactor design, and it is usually less than a millisecond in light water reactors [Hetrick, 1993].

The adiabatic Nordheim-Fuchs model also gives an approximation to the pulse shape under a prompt critical event. More precisely, the pulse shape is given by

Equation A-4:
$$P(t) = P_{max} \operatorname{sech}^2\left(\frac{(\Delta\rho-\beta)(t-t_{max})}{2\Lambda}\right)$$

where P_{max} and t_{max} are the maximum power and the time at which the maximum is obtained, respectively. Although the adiabatic Nordheim-Fuchs model is very simple, the pulse widths and pulse shapes provided by Equation A-3 and Equation A-4 are in fair agreement with those obtained from state-of-the-art three-dimensional core kinetics analyses of control rod ejection accidents and control rod drop accidents. This is illustrated in section 2.2.1 of the report.

Finally, the adiabatic Nordheim-Fuchs model also gives a simple analytical approximation to the pulse amplitude (in units of watt per fuel mass)

$$P_{max} \approx -\frac{c_f(\Delta\rho-\beta)^2}{2\Lambda\left(\frac{\partial\rho}{\partial T_f}\right)}$$

Equation A-5:

Here, c_f is the specific heat capacity of the fuel material, and $\partial\rho/\partial T_f$ is the fuel temperature coefficient, as defined in Equation A-2. These material properties are thus of fundamental importance to the pulse amplitude. The adiabatic Nordheim-Fuchs model also gives a simple approximation to the total energy deposition in the fuel under the power pulse

$$E_{tot} \approx -\frac{2c_f(\Delta\rho-\beta)}{\partial\rho/\partial T_f}$$

Equation A-6:

where E_{tot} is in units of joule per fuel mass. It should be noted that, while the prompt reactivity insertion, $\Delta\rho-\beta$, is quadratic in the expression for P_{max} in Equation A-5, it is only linear in the expression for total energy deposition in Equation A-6. Hence, the peak power increases more quickly with respect to reactivity insertion than the deposited energy. The reason is that if the reactivity addition is larger, the pulse is also terminated more quickly; see Equation A-3.

It is clear from the Nordheim-Fuchs relations in Equation A-3 - Equation A-6 that the difference $\Delta\rho-\beta$ is a key parameter for the power pulse that results from a prompt criticality accident. The reactivity insertion, $\Delta\rho$, depends on the accident scenario; see section 2. The fraction of delayed neutrons, on the other hand, depends on the isotopic composition of the fuel, as shown in Table A-1. In a light water reactor loaded with fresh UO_2 fuel, about 90% of the fissions take place in ^{235}U , and the remaining part in ^{238}U . The effective fraction of delayed neutrons is then about 0.0077. This number decreases with increasing burnup, as ^{235}U is consumed and fissioning of plutonium isotopes becomes significant. The rate at which β declines with increasing burnup depends inversely on the as-fabricated enrichment.

Appendix B Pulse reactor tests on pre-irradiated LWR fuel rods

This appendix summarizes RIA simulation tests that have been conducted in dedicated pulse reactors on pre-irradiated LWR fuel rods and reported in literature up to October 2022. Similar presentations of RIA simulation tests on un-irradiated UO₂ fuel rods can be found in the reviews by MacDonald et al. [1980], Ishikawa and Shiozawa [1980], and Ishikawa et al. [1989]. Tests on un-irradiated MOX fuel have been reported by Abe et al. [1992], and similar work on un-irradiated ROX fuel can be found in [Nakamura et al, 2003a; Nakamura et al, 2003b].

All data presented below are taken from open-literature sources. It should be made clear that data reported for a particular test can vary from one literature source to another. For instance, it is not unusual that preliminary data are presented at conferences, and later adjusted as the experiments are more carefully evaluated. Precedence has therefore been given to the latest published data, in those cases where conflicting values have been reported in literature. It should also be remarked that a major revision of reported fuel enthalpies for pre-irradiated fuel, tested in the NSRR before 2003, has recently been published [Udagawa et al, 2014]. These revised enthalpies are presented here. In many cases, they differ significantly from values reported earlier.

All reported fuel enthalpies are axial peak, radial average values for the fuel pellets, and they are calculated with respect to a reference temperature of 273K; see section 1.2. Since all power pulses in the summary are initiated from zero or near zero power, the initial fuel temperature is very close to the coolant temperature. Hence, the fuel enthalpy *increase* under the pulse test can be calculated by subtracting the reported peak fuel enthalpy with the initial fuel enthalpy, under the assumption that the initial fuel and coolant temperatures are equal. In case initial coolant temperature is different from Room Temperature, e.g., 280°C (553K) in CABRI, the initial enthalpy should be subtracted from the peak fuel enthalpy to obtain the enthalpy rise (ΔH): the enthalpy rise is the one generating the actual loading to be applied by the pellet to the cladding.

It should be mentioned that tests have been done also with power pulses that simulate the conditions of RIAs at full reactor power [Katanishi & Ishijima, 1995]. These tests, carried out on un-irradiated UO₂ fuel rods, are not considered here.

B.1 SPERT-CDC and TREAT tests

The SPERT-CDC test program included tests on both un-irradiated test rods and rods that were pre-irradiated in the Engineering Test Reactor to rod average burnups in the range of 1 to 32 MWd(kgU)⁻¹ then tested in the SPERT-CDC test reactor (Special Power Excursion **R**ector – Capsule Driver Core) in Idaho Falls. A total of ten pre-irradiated rodlets were tested in a sealed capsule, which was equipped with a pressure transducer and contained stagnant water at atmospheric pressure and room temperature. The rodlets were not instrumented, but the pressure transducer in the test capsule was used to detect coolant pressure spikes. In this way, it was possible to determine the approximate time and fuel enthalpy at which a test rod failed.

The tests on pre-irradiated fuel simulated the conditions of a BWR during cold start-up, and the thermal-mechanical behaviour of BWR-type UO₂ test rodlets was investigated. The coolant was stagnant water at atmospheric pressure and 298K. The pulse widths were in the range of 13 to 31 ms [MacDonald et al, 1980]. Each test rod contained a short, 132 mm fuel length, cladding tube of 10% cold-worked Zircaloy-2. The UO₂ fuel pellet density was about 94% of theoretical density, and the enrichment was 7 wt% ²³⁵U. Two different fuel rod designs were used: GEX-type with a cladding outer diameter of 7.94 mm and GEP-type with a diameter of 14.29 mm. The small-diameter GEX-rods were designed to increase the attainable energy deposition in the RIA simulation facility, and their cladding wall thickness and fuel-cladding gap were reduced in proportion to the cladding diameter.

The total deposited energies for the pre-irradiated test rods in SPERT-CDC, along with their respective burnups, are presented in Table B-1. The energy deposition was determined by measuring the activity of a cobalt wire located in the vicinity of the test capsule. The technique provides the total energy

deposition during the transient and has an accuracy of $\pm 12\%$. Roughly 10 to 20% of the energy deposition occurs after the power pulse, i.e., during low powers prior to reactor scram. This delayed energy deposition does not contribute to the peak fuel enthalpy. The radially averaged peak fuel enthalpy was therefore estimated using a correction of 17% to account for the delayed energy deposition [MacDonald et al, 1980].

The Transient Reactor Test (TREAT) facility was designed and built in the late 1950s at Argonne National Laboratory West campus (ANL-W) located in the Arco Desert, west of Idaho Falls, Idaho, to provide a transient reactor for safety experiments on samples of reactor fuels. It first operated in 1959. Throughout its history, experiments conducted in TREAT have been important in establishing the behaviour of a wide variety of reactor fuel elements under conditions predicted to occur in reactor accidents ranging from mild off-normal transients to hypothetical core disruptive accidents. Among many others, TREAT was used to test light water reactor (LWR) elements in a steam environment to obtain fission product release data under meltdown conditions. TREAT studies, but mostly SPERT-CDC studies, have been used to evaluate behaviour of low to medium burnup LWR fuels under reactivity-initiated accident (RIA) conditions [MacDonald et al, 1980].

Table B-1: SPERT-CDC tests on pre-irradiated fuel rods. Data compiled from [MacDonald et al, 1980; Meyer, 2006].

| Test ID | Fuel burnup [MWd(kgU) ⁻¹] | Clad oxide thickness [μm] | Pulse width [ms] | Peak fuel enthalpy [cal(gUO ₂) ⁻¹ /J(gUO ₂) ⁻¹] | Failure enthalpy [cal(gUO ₂) ⁻¹ /J(gUO ₂) ⁻¹] | Fuel loss [%] |
|------------------------------------|---|--|-----------------------|---|---|--------------------|
| 567 | 3.1 | 0 | 18 | 214/896 | 214/896 | NA |
| 568 | 3.8 | 0 | 24 | 161/674 | 147/615 | NA |
| 569 | 4.1 | 0 | 14 | 282/1181 | 282/1181 | NA |
| 571 | 4.6 | 0 | 31 | 137/574 | Survived | – |
| 684 | 13 | 0 | 20 | 170/712 | Survived | – |
| 685 | 13 | 0 | 23 | 158/662 | Survived | – |
| 703 | 1.1 | 0 | 15 | 163/682 | Survived | – |
| 709 | 1.0 | 0 | 13 | 202/846 | 202/846 | NA |
| 756 | 32 | 65 | 17 | 143/600 | 143/600 | 0 |
| 859 | 32 | 65 | 16 | 154/645 | 85/356 | >0 |
| NA: Data are not available. | | | | | | |
| ANT International, 2016 | | | | | | |

Several of the low-burnup rods failed during or following the power pulse. Also, both of the failed high-burnup rods (rods 756 and 859) exhibited brittle-type cladding fracture. Rod 756 failed for a peak fuel enthalpy of 143 cal/(gUO₂)⁻¹ (600 J(gUO₂)⁻¹), whereas rod 859 failed at 85 cal/(gUO₂)⁻¹ (356 J(gUO₂)⁻¹). A large hydride blister was found in rod 859 despite the very low burnup of the fuel rodlet (32 MWd(kgU)⁻¹). The cause of failure for these two rods was attributed to heavy accumulations of zirconium hydride during the non-prototypical pre-test irradiation conditions in ETR. Nontypical test conditions could also have contributed to the cladding failure, i.e., the low initial cladding temperatures in combination with the narrow power pulses, which were utilised in the SPERT-CDC tests, resulted in relatively low cladding temperatures at the time of maximum cladding stresses.

The direct applicability of the SPERT-CDC test results to LWR RIA conditions must be questioned since the design of the test rodlets is different from that of today's light water reactor fuel. In addition, the test rods were pre-irradiated in the ETR facility at very high linear heat generation rates, 46–67 kWm⁻¹, resulting in fuel restructuring and even central hole formation. Hence, these tests are not prototypical of fuel rods irradiated in commercial light water reactors.

Appendix C (Information from ZIRAT18 STR on Mechanical Testing Vol. II)

C.1 Mechanical testing techniques

Together with the strain rate the heating rate parameter should be considered as well: it has an impact on the mechanical properties evolution (through H dissolution rate and irradiation defects annealing rate, etc.). Performing mechanical properties tests at constant temperature is easier but likely insufficiently realistic. That is the limitation of most of the mechanical tests available.

Various scenarios for RIA events are described in earlier sections. Table C-1, Table C-2, and Table C-3 tabulate summaries. The cladding is generally presumed to experience two stages of mechanical loading which both can lead to plastic deformation and possible cladding rupture. The first phase is controlled by pellet clad mechanical interaction (PCMI) which is dominated by expansion of the fuel pellet against the inner cladding surface. Particularly at burnups higher than about 40 GWd/MT, the absence of a pellet-to-cladding gap and the presence of strong pellet-to-cladding chemical and mechanical bonding causes the cladding to be stretched in both the hoop (circumferential) and axial directions. The ratio of stresses in the two directions (σ_a/σ_h) is not precisely known; in the ideal case it might be close to 1 (i.e., 1/1) but in practice the ratio probably varies between 1 and 2. It is important to note that this is biaxial loading, not uniaxial loading as often occurs in other situations.

It must be noted as well that the mechanical testing techniques available today do not enable simulating all the thermomechanical phenomena at work during the PCMI phase of an RIA. Various artefacts prevent the test results to be used directly to define, for instance, an RIA failure criterion. In-pile RIA tests are still necessary.

Nevertheless, mechanical testing techniques are useful, in a relative way, to rank the different types of claddings against their resistance when they are loaded rapidly, mechanically, and thermally and to interpretate the in-pile RIA tests. To better transfer the mechanical property tests results, finite element analysis of the testing devices is often required to account for e.g., the actual stress biaxial ratio, the friction coefficients between the specimen and the loading fixtures, the elasticity of the testing device framework, etc...

Table C-1: RIA mechanical loading conditions

| |
|--|
| Phase 1 – PCMI (pellet-cladding-mechanical interaction) |
| <ul style="list-style-type: none"> - Roughly equal biaxial (hoop +axial) stress - $\sigma(a)/\sigma(h) = 1$ ideally (or 1–2 in practice) - Strain rate high – 1–5 / s - Plane strain - Short duration – few tens of milliseconds |
| Phase 2 – clad ballooning |
| <ul style="list-style-type: none"> - High temperature and fission gas pressure |
| ANT International, 2016 |

Table C-2: RIA temperature conditions

| PWR – control rod ejection |
|--|
| <ul style="list-style-type: none"> - Hot Zero Power (HZP) - 200°C < T < 800°C - Average or optimum-- 400°C ?? |
| BWR – control rod drop |
| <ul style="list-style-type: none"> - Cold Zero Power (CZP) - 30°C < T < 300°C - Average or optimum– 100°C ?? |
| ANT International, 2016 |

Table C-3: RIA mechanical testing techniques

| Hoop to axial stress ratios |
|--|
| <ul style="list-style-type: none"> - 0/1 – uniaxial tension - 1/0 – open end burst test - 2/1 – closed end burst test - 1/1 – ideal for RIA stage 1 |
| Specimens |
| <ul style="list-style-type: none"> - Many used for testing and analysis - Not all apply directly - Some axial, some hoop, some conventional from other applications |
| ANT International, 2016 |

Another key parameter is the ratio of strains in the two directions. An approximate conversion between the two is [Cazalis et al, 2005]:

Equation C-1:

$$\frac{\varepsilon_{zz}}{\varepsilon_{\theta\theta}} = \frac{\left(\frac{2\sigma_{zz}}{\sigma_{\theta\theta}}\right) - 1}{2 - \frac{\sigma_{zz}}{\sigma_{\theta\theta}}}$$

This first phase is characterized by high heating rates in the cladding of about 10^3 K s^{-1} and high strain rates on the order of 1 s^{-1} . The cracks initiated by the hoop tensile stresses during the PCMI phase of the RIA transient conditions are observed to form along the length of the cladding tube (i.e., in the axial direction) and to propagate primarily through the wall.

The heating pulse lasts a few tens of milliseconds. Many references to RIA scenarios exist. Three early ones are [de Betou et al, 2004; Desquines et al, 2004; Le Saux et al, 2007].

Cladding temperature is very important, particularly for high burnup fuel where hydride concentration can be in the 100–1000 ppm range. As discussed earlier, for PWRs the most severe accident occurs for a control rod ejection situation when the core is at hot zero power conditions [Nakajima et al, 2002]. Therefore, the temperature starts at about 200°C (553K); during the millisecond pulse the cladding temperature rises to as high as 600°C (873K), [Desquines et al, 2004], or even higher (Figure C-1), [de Betou et al, 2004]. The optimum testing temperature is uncertain, but 400°C (673K) would seem to be a minimum. For BWRs the most severe condition is a control rod drop (CRDA) during cold zero power condition, [Nakajima et al, 2002], where the cladding starts at 30–100°C (303–373K). Increases in temperature are expected to be small, as evidenced by simulations conducted at the NSRR in Japan [Nakamura et al, 2000], [Nakamura et al, 2003], [Vitanza & Conde, 2004]. There it was shown, under conditions similar to a BWR CRDA, that cladding temperature during the pulse remained less than 100°C (373K).

References

- Abe H., et al., *Development of advanced expansion due to compression (A-EDC) test method for safety evaluation of degraded nuclear fuel cladding materials*, Journal of Nuclear Science and Technology, 2015, 52(10): pp. 1232-1239.
- Abe T., Nakae N., Kodato K. and Matsumoto M., *Failure behaviour of plutonium-uranium mixed oxide fuel under reactivity initiated accident condition*, Journal of Nuclear Materials, 1992, 188: pp. 154-161.
- Adamson M. G., Aitken E. A. and Caputi R. W., *Experimental and thermodynamic evaluation of the melting behaviour of irradiated oxide fuels*, Journal of Nuclear Materials, 1985, 130: pp. 349-365.
- Adamson R. B, Garzarolli F., Patterson C., Rudling P. and Strasser A., *ZIRAT14/IZNA9 Annual Report*, ANT International, Mölnlycke, Sweden, 2009.
- Adamson R. B., Coleman K., Mahmood S. T. and Rudling P., *Mechanical testing of Zirconium alloys, ZIRAT18/IZNA13 Special Topic Report, Vols. I and II*, Advanced Nuclear Technology International, Mölnlycke, Sweden, 2013/2014.
- Ade B., et al., *Safety and regulatory issues of the thorium fuel cycle*, Report ORNL/TM/2013/543 (NUREG/CR-7176), Oak Ridge National Laboratory, Oak Ridge, TN, USA, 2014.
- Agee L. J., Dias A. F., Eisenhart L. D. and Engel R. E., *Realistic scoping study of reactivity insertion accidents for a typical PWR and BWR core*, Proc. CSNI specialist meeting on transient behaviour of high burnup fuel, pp. 291-304, Cadarache, France, September 12-14, 1995.
- Amaya M., Sugiyama T., Nagase F. and Fuketa T., *Fission gas release in BWR fuel with a burnup of 56 GWd/t during simulated reactivity initiated accident (RIA) condition*, Journal of Nuclear Science and Technology, 2008, 45(5): pp. 423-431.
- Amaya M., Udagawa Y., Narukawa T., Mihara T. and Sugiyama T., *Behavior of high burnup advanced fuels for LWR during design-basis accidents*, 2015. In: TopFuel-2015, Zürich, Switzerland: European Nuclear Society, pp. 10-18, September 13-17, 2015.
- Amaya M., et al. *Behavior of high-burnup advanced LWR fuels under accident conditions*, 2016. In: TopFuel 2016, Boise, ID, USA: American Nuclear Society, pp. 53-62, September 11-15, 2016.
- Andersson T. and Wilson A, *Ductility of Zircaloy canning tubes in relation to stress ratio in biaxial testing*. In: Zirconium in the nuclear industry; 4th international symposium: J.H. Schemel and T.P. Papazoglou, Eds., American Society for Testing and Materials, ASTM STP-681, pp. 60-71, 1979.
- Arborelius J., et al. *Advanced Doped UO₂ Pellets in LWR Applications*, Journal of Nuclear Science and Technology, 2006, 43(5): pp. 967-976.
- [R.] Armstrong, *Results of the CHF-SERRTA in-pile transient boiling experiments at TREAT*, ANS TOPFUEL 2021:].
- Arséne S. and Bai J. B., *A new approach to measuring transverse properties of structural tubing by a ring test*, Journal of Testing and Evaluation (JTEVA), 1996, 24(6): pp. 386-391.
- Asmolov V. and Yegorova L., *The Russian RIA research program: Motivation, definition, execution and results*, Nuclear Safety, 1996, 37(4): pp. 343-371.
- Azuma M., Taniguchi A., Hotta A. and Ohta T., *Assessment on integrity of BWR internals against impact load by water hammer under conditions of reactivity initiated accidents*, Nuclear Technology, 2005, 149: pp. 243-252.
- Backman, K., L. Hallstadius and G. Roennberg (2010), *Westinghouse Advanced Doped Pellet – Characteristics and Irradiation Behaviour*, IAEA Technical committee meeting on advanced fuel pellet materials and fuel rod design for water cooled reactors, 23-26 November 2009, Villigen, Switzerland, IAEA-TECDOC-1654, pp. 117-126.

- Bales M. and Clifford P, *Proposed Changes in Regulation for LOCA and RIA in the US*, Fuel Safety Research Meeting, Mito, Japan, October 18–19, 2016.
- Bales M., et al. *The NEA Framework for Irradiation Experiments (FIDES): A New Future for International Collaboration on Nuclear Fuel Research*, Top Fuel 2022, October 9-13, 2022, Raleigh, NC, Proceedings pp 719-721
- Balourdet M. and Bernaudat C., *Tensile properties of Zircaloy-4 cladding submitted to fast transient loading*, 1995. In: CSNI specialist meeting on transient behaviour of high burnup fuel, Cadarache, France: OECD Nuclear Energy Agency, NEA/CSNI/R(95)22, pp. 417-431, September 12-14, 1995.
- Balourdet M., et al. *The PROMETRA programme: Assessment of mechanical properties of Zircaloy-4 fuel cladding during an RIA*, 1999. In: 15th international conference on structural mechanics in reactor technology (SMiRT-15), Seoul, Korea, Vol II, pp. 485-492, August 15-20, 1999.
- Bates D.W., et al. *Influence of specimen design on the deformation and failure of Zircaloy cladding*. In: ANS topical meeting on light water reactor fuel performance, Park City, Utah, USA: American Nuclear Society, pp. 296-305, April 10-13, 2000.
- Bernaudat C. and Pupier P., *A new analytical approach to study the rod ejection accident in PWRs*, Water Reactor Fuel Performance Meeting, Japan, October, 2005.
- Berthoud G., *Vapor explosions*, Annular Review of Fluid Mechanics, 2000, 32: pp. 573-611.
- Bess D.J., et al. *Narrowing transient testing pulse widths to enhance LWR RIA experiment design in the TREAT facility*, Annales of Nuclear Energy, Vol. 124, February 2019, pp 548-571
- Bessiron V., *The PATRICIA program on clad to coolant heat transfer during reactivity initiated accidents*. In: Tenth international topical meeting on nuclear reactor thermal hydraulics (NURETH-10), Seoul, Korea, October 5-9, 2003.
- Bessiron V., *Clad-to-coolant heat transfer during a RIA transient: Analysis of the PATRICIA experiments, modelling and applications*. In: Fuel safety research meeting, Tokyo, Japan, March 1-2, 2004.
- Bessiron V., *Modelling of clad to coolant heat transfer for RIA applications*, Journal of Nuclear Science and Technology, 2007, 44(2): pp. 211-221.
- Bodansky D., *Nuclear Energy: Principles, practices and prospects*. 2nd ed., New York: Springer AIP Press, 2004.
- Bogdanov V.N., et al. *Irradiating complex on BGR reactor for simulation accidents of RIA type*. In: Seventh international conference on nuclear criticality and safety, Tokai, Japan: Japan Atomic Energy Research Institute, pp. 770-772, October 20-24, 2003.
- Bourguignon D., *The new CABRI water loop: Detailed description of the new water loop and of the specific new zircaloy in-core experimental cell*. In: 10th Meeting of the International Group on Research Reactors, Gaithersburg, MD, USA, September 12-16, 2005.
- Carbajo J., Yoder G., Popovb S. and Ivanov V., *A review of the thermophysical properties of MOX and UO₂ fuels* Journal of Nuclear Materials, 2001, 299: pp. 181-198.
- Carassou S. et al, *Ductility and Failure Behaviour of both Unirradiated and Irradiated Zircaloy-4 Cladding Using Plane Strain Tensile Specimens*, OECD/NEA Workshop, Nuclear Fuel Behaviour during RIA, Paris, Sept. 2009.
- Carey V. P., *Liquid-vapor phase-change phenomena: An introduction to the thermophysics of vaporization and condensation processes in heat transfer equipment*, 2nd ed., Taylor & Francis, Washington, USA, 2007.
- Carmack W.J., et al., *Inert matrix fuel neutronic, thermal-hydraulic, and transient behavior in a light water reactor*. Journal of Nuclear Materials, 2006, 352(1-3): pp. 276-284.

Nomenclature

The symbols and abbreviations used in this report are listed below, together with a brief explanation to the notation. The symbols used conform as far as possible to prevalent nomenclature in international literature. Throughout the text, all mathematical symbols are printed in italic. The international system of units (SI) is applied.

Latin symbols:

| | | |
|--------------|---|--|
| c_f | Fuel specific heat capacity | [J(gK) ⁻¹] |
| d_{32} | Mean diameter (volume-to-surface diameter) | [m] |
| E_{tot} | Total energy deposited to the fuel | [J(gUO ₂) ⁻¹] |
| h_f | Fuel pellet specific enthalpy (radial average) | [Jg ⁻¹] |
| k_{eff} | Effective neutron multiplication factor | [-] |
| k_{∞} | Infinite lattice multiplication factor | [-] |
| L_o | Test specimen gauge length | [m] |
| P_{max} | Power pulse amplitude | [W(gUO ₂) ⁻¹] |
| t | Time | [s] |
| T | Temperature | [K] |
| T_0 | Reference temperature, at which $h_f=0$. Here, $T_0=273$ K | [K] |
| T_f | Fuel temperature | [K] |
| T_m | Moderator temperature | [K] |
| T_s | Solidus (melting) temperature | [K] |
| W_o | Test specimen gauge section with | [m] |

Greek symbols:

| | | |
|------------------------------|---|--------|
| α_m | Moderator void volume fraction | [-] |
| β | Effective delayed neutron fraction | [-] |
| ΔP | Fuel rod internal gas overpressure | [Pa] |
| $\varepsilon_{\theta\theta}$ | Hoop (circumferential) strain | [-] |
| ε_{zz} | Axial (longitudinal) strain | [-] |
| Λ | Effective neutron lifetime | [s] |
| ρ | Reactivity | [-] |
| σ | Uniaxial or effective stress | [Pa] |
| $\sigma_{\theta\theta}$ | Hoop (circumferential) stress | [Pa] |
| σ_{zz} | Axial (longitudinal) stress | [Pa] |
| τ | Pulse width (Full width at half maximum - FWHM) | [s] |

List of Abbreviations

| | |
|-------|--|
| ACPR | Annular Core Pulse Reactor |
| AECL | Atomic Energy of Canada Limited |
| AISI | American Iron and Steel Institute |
| ANL | Argonne National Laboratory (USA) |
| ANSI | American National Standards Institute |
| ANT | Advanced Nuclear Technology |
| AOA | Axial Offset Anomaly |
| AOO | Anticipated Operating Occurrence |
| AREVA | French Equipment Manufacturer |
| ASEA | Allmänna Svenska Elektriska Aktiebolaget (General Swedish Electrical Limited Company) |
| ASME | American Society of Mechanical Engineers |
| ATF | Accident Tolerant Fuel |
| ATR | Advanced Thermal Reactor |
| AUC | Ammonium uranocarbonate |
| B&W | Babcock & Willcox |
| BA | Burnable Absorber |
| BCC | Body Centred Cubic |
| BIGR | Fast Impulse Graphite Reactor (Russia) |
| BNFL | British Nuclear Fuels Limited |
| BOC | Beginning of Cycle |
| BOP | Balance of Plant |
| BR3 | Belgian Reactor 3 (Belgium) |
| BWR | Boiling Water Reactor |
| CANDU | Canadian Deuterium Uranium |
| CASL | Consortium for Advanced Simulation of LWRs |
| CE | Combustion Engineering |
| CEA | Commissariat à l'Énergie Atomique et aux Énergies Alternatives (French atomic energy commission) |
| CILC | CRUD Induced Localized Corrosion |
| CIP | CABRI International Program |
| CIPS | CRUD Induced Power Shift |
| CP | Corrosion Product |
| CR | Control Rod |
| CRDA | Control Rod Drop Accident |
| CREA | Control Rod Ejection Accident |
| CRUD | Chalk River Unidentified Deposits |
| CSED | Critical Strain Energy Density |
| CVCS | Chemical and Volume Control System |
| CWSR | Cold Work and Stress Relieved |
| CZP | Cold Zero Power |
| DNB | Departure from Nuclear Boiling |
| E110 | Cladding material used in VVER fuel rods (Zr-1.0Nb by wt%) |
| ECBE | Effective Control Blade Exposure |
| EDC | Expansion Due to Compression |
| EDF | Electricité de France |
| EFID | Effective Full Insertion Days |
| ELS | Extra-Low Sn |
| EOC | End Of Cycle |
| EPRI | Electric Power Research Institute (USA) |
| ESSC | Enhanced Spacer Shadow Corrosion |
| ETR | Engineering Test Reactor (USA) |
| FA | Fuel Assembly |
| FCI | Fuel-Coolant Interaction |
| FGR | Fission Gas Release |
| FP | Fission Product |
| FRED | Fuel Reliability Data Base |

NUCLEAR FUEL BEHAVIOUR UNDER RIA CONDITIONS

| | |
|--------|---|
| FRI | Fuel Reliability Indicators |
| FWHM | Full Width at Half Maximum |
| GC | Guide Channels |
| GE | General Electric |
| GNF | Global Nuclear Fuel |
| GT | Guide Tubes |
| GTRF | Grid-To-Rod Fretting |
| HANA-4 | Cladding alloy developed by KAERI (Zr-1.5Nb-0.4Sn-0.2Fe-0.1Cr by wt%) |
| HAZ | Heat Affected Zone |
| HBS | High Burnup Structure |
| HCP | Hexagonal Close-Packed |
| HFE | Healthy Fuel Examinations |
| HFP | Hot Full Power |
| HM | Heavy Metal |
| HPA | High Performance Alloy |
| HPU | Hydrogen Pick-Up |
| HPUF | Hydrogen Pick-Up Fraction |
| HTP | High Thermal Performance |
| HWC | Hydrogen Water Chemistry |
| HZP | Hot Zero Power |
| IAEA | International Atomic Energy Agency (Austria) |
| IASCC | Irradiation Assisted Stress Corrosion Cracking |
| ID | Inner Diameter |
| IGR | Impulse Graphite Reactor (Kazakhstan) |
| IGSCC | Intergranular Stress Corrosion Cracking |
| IMF | Inert Matrix Fuel |
| INPO | Institute of Nuclear Power Operations |
| IRI | Incomplete Rod Insertion |
| IRSN | Institut de Radioprotection et de Sûreté Nucléaire (France) |
| JAEA | Japan Atomic Energy Agency (formerly JAERI) |
| JAERI | Japan Atomic Energy Research Institute (now JAEA) |
| JMTR | Japanese Material Test Reactor |
| KAERI | Korean Atomic Energy Research Institute |
| KKL | KernKraftwerk Leibstadt |
| KWU | KraftWerkUnion |
| LCC | LWR Coolant Chemistry |
| LHGR | Linear Heat Generation Rate |
| LME | Liquid Metal Embrittlement |
| LMFBR | Liquid Metal Fast Breeder Reactor |
| LOCA | Loss of Coolant Accident |
| LWR | Light Water Reactor |
| M5 | Cladding trademark of Framatome ANP (Zr-1.0Nb-0.13O by wt%) |
| MBT | Modified Burst Test |
| MCP | Main Circulating Pump |
| MDA | Mitsubishi Developed Alloy (Zr-0.8Sn-0.5Nb-0.2Fe-0.1Cr by wt%) |
| MIMAS | MIcronised MAsterblend |
| M-MDA | Modified Mitsubishi Developed Alloy (Zr-0.5Sn-0.5Nb-0.3Fe-0.4Cr by wt%) |
| MOX | Mixed Oxide (UO ₂ /PuO ₂) |
| MPS | Missing Pellet Surface |
| NDA | New Developed Alloy (Zr-1.0Sn-0.27Fe-0.16Cr-0.1Nb-0.01Ni by wt%) |
| NEI | Nuclear Energy Institute |
| NFIR | Nuclear Fuel Industry Research |
| NG | Nuclear Grade |
| NMCA | Noble Metal Chemical Addition |
| NPD | Nuclear Power Demonstration |
| NPP | Nuclear Power Plant |
| NRC | Nuclear Regulatory Commission |
| NRX | Test reactor (Canada) |
| NSRR | Nuclear Safety Research Reactor (Japan) |

NUCLEAR FUEL BEHAVIOUR UNDER RIA CONDITIONS

| | |
|--------|--|
| NSSS | Nuclear Steam Supply System |
| NWR | Normal Water Chemistry |
| OD | Outer Diameter |
| OECD | Organisation for Economic Co-operation and Development |
| OLNC | On-Line Noble Chemistry |
| OPG | Ontario Power Generation company |
| OTSG | Once-Through Steam Generators |
| PBF | Power Burst Facility (USA) |
| PCI | Pellet Cladding Interaction |
| PCMI | Pellet Cladding Mechanical Interaction |
| PGS | Pickering Generation Station |
| PSD | Power Spectral Density |
| PSU | Pennsylvania State University (USA) |
| PWR | Pressurised Water Reactor |
| PWSCC | Pressurised Water Stress Corrosion Cracking |
| QA | Quality Assurance |
| QC | Quality Control |
| RBMK | Russian type, graphite moderated, pressure tube light water reactor |
| RCCA | Rod Cluster Control Assembly |
| RCP | Reactor Coolant Pump |
| RDA | (Control) Rod Drop Accident |
| REA | (Control) Rod Ejection Accident |
| REP | Réacteurs à Eau Pressurisée (Pressurized water reactor) |
| RHL | Rapid Heating and Loading |
| RIA | Reactivity Initiated Accident |
| RIL | (Control) Rod Insertion Limit |
| RISA | Radiation Induced Surface Activation |
| ROX | Rock-like Oxide |
| RST | Ring Stretch Test |
| RXA | Recrystallised Annealed |
| SBR | Short Binderless Route |
| SCC | Stress Corrosion Cracking |
| SCI | Shadow Corrosion Induced |
| SED | Strain Energy Density |
| SEM | Scanning Electron Microscopy |
| SG | Steam Generator |
| SI | Le Système Internationale d'unités (The international system of units) |
| SL-1 | Stationary Low Power Plant No. 1 (USA) |
| SNB | Subcooled Nucleate Boiling |
| SP | Spacer Position |
| SPERT | Special Power Excursion Reactor (USA) |
| SPP | Second Phase Particles |
| SR | Stress Relieved |
| SRA | Stress Relieved Annealed |
| SS | Stainless Steel |
| STR | Special Topic Report |
| TCO | Cladding outer surface temperature |
| TIG | Tungsten Inert Gas |
| TRIGA | Training, Research, Isotopes General Atomics |
| UFC | Ultrasonic Fuel Cleaning |
| US NRC | United States Nuclear Regulatory Commission (USA) |
| UT | Ultrasonic Testing |
| WANO | World Association of Nuclear Operators |
| wppm | Weight Parts Per Million |
| VVER | Russian type pressurized water reactor |
| ZIRLO | ZIRconium Low Oxidation |

Unit conversion

| TEMPERATURE | | |
|--|---|-------------------------|
| $^{\circ}\text{C} + 273.15 = \text{K}$ | $^{\circ}\text{C} \times 1.8 + 32 = ^{\circ}\text{F}$ | |
| T(K) | T($^{\circ}\text{C}$) | T($^{\circ}\text{F}$) |
| 273 | 0 | 32 |
| 289 | 16 | 61 |
| 298 | 25 | 77 |
| 373 | 100 | 212 |
| 473 | 200 | 392 |
| 573 | 300 | 572 |
| 633 | 360 | 680 |
| 673 | 400 | 752 |
| 773 | 500 | 932 |
| 783 | 510 | 950 |
| 793 | 520 | 968 |
| 823 | 550 | 1022 |
| 833 | 560 | 1040 |
| 873 | 600 | 1112 |
| 878 | 605 | 1121 |
| 893 | 620 | 1148 |
| 923 | 650 | 1202 |
| 973 | 700 | 1292 |
| 1023 | 750 | 1382 |
| 1053 | 780 | 1436 |
| 1073 | 800 | 1472 |
| 1136 | 863 | 1585 |
| 1143 | 870 | 1598 |
| 1173 | 900 | 1652 |
| 1273 | 1000 | 1832 |
| 1343 | 1070 | 1958 |
| 1478 | 1204 | 2200 |

| Radioactivity | | |
|---------------|------------------------------------|--|
| 1 Sv | = 100 Rem | |
| 1 Ci | = 3.7×10^{10} Bq = 37 GBq | |
| 1 Bq | = 1 s^{-1} | |

| MASS | |
|-------|------|
| kg | lbs |
| 0.454 | 1 |
| 1 | 2.20 |

| DISTANCE | |
|---------------------|----------|
| x (μm) | x (mils) |
| 0.6 | 0.02 |
| 1 | 0.04 |
| 5 | 0.20 |
| 10 | 0.39 |
| 20 | 0.79 |
| 25 | 0.98 |
| 25.4 | 1.00 |
| 100 | 3.94 |

| PRESSURE | | |
|----------|------|-------|
| bar | MPa | psi |
| 1 | 0.1 | 14 |
| 10 | 1 | 142 |
| 70 | 7 | 995 |
| 70.4 | 7.04 | 1000 |
| 100 | 10 | 1421 |
| 130 | 13 | 1847 |
| 155 | 15.5 | 2203 |
| 704 | 70.4 | 10000 |
| 1000 | 100 | 14211 |

| STRESS INTENSITY FACTOR | |
|-------------------------|--------------------------|
| MPa $\sqrt{\text{m}}$ | ksi $\sqrt{\text{inch}}$ |
| 0.91 | 1 |
| 1 | 1.10 |

| ENTHALPY | |
|---------------------------|--------------|
| Cal_{th}/g | J/g |
| 1.0 | 4.184 |
| 0.239 | 1.0 |

Cal_{th} – applied over this document refer to the thermochemical calories determined in calorimetry